Journal of Organometallic Chemistry 696 (2011) 1496–1509

Contents lists available at ScienceDirect

Journal of Organometallic Chemistry

journal homepage: www.elsevier.com/locate/jorganchem

The preparation, spectroscopy, structure and electrochemistry of some $[\mathrm{Co}(\eta^4\text{-}\mathrm{C_4Ph_4})(\eta^5\text{-}\mathrm{C_5H_4R})]$ complexes

Paul O'Donohue [a], C. John McAdam [b,*], Donagh Courtney [a], Yannick Ortin [a], Helge Müller-Bunz [a], Anthony R. Manning [a], Michael J. McGlinchey [a], Jim Simpson [b]

[a] *School of Chemistry and Chemical Biology, University College Dublin, Belfield, Dublin 4, Ireland.*
[b] *Department of Chemistry, University of Otago, PO Box 56, Dunedin 9054, New Zealand*

ARTICLE INFO

Article history:
Received 1 November 2010
Received in revised form
15 December 2010
Accepted 20 December 2010

Keywords:
Cobalt
Tetraphenylcyclobutadiene
Ferrocenyl

ABSTRACT

$[\mathrm{Co}(\eta^4\text{-}\mathrm{C_4Ph_4})(\eta^5\text{-}\mathrm{C_5H_4R})]$ ($\mathrm{R = CO_2Me}$, **2**; and CHO, **3**), prepared by the reactions of $[\mathrm{Co}(\eta^5\text{-}\mathrm{C_5H_4R})(\mathrm{PPh_3})_2]$ with $\mathrm{Ph_2C_2}$, were used as precursors for complexes where $\mathrm{R = CH_2OH}$, **4**; $\mathrm{CH_2Cl}$, **5**; $\mathrm{CH_2P(O)(OEt)_2}$, **6**; $\mathrm{CH_2PPh_3^+}$, [**7**]$^+$; C(O)Fc, **8** (Fc = ferrocenyl); $\mathrm{CFc_2OH}$, **9**; $\mathrm{CH{=}C(CN)_2}$, **10**; *syn* and *anti*-$\mathrm{CH{=}NNH{-}C_6H_3(NO_2)_2\text{-}2,4}$, **11**; CH(Fc)OH, **12**; $\mathrm{CHFc^+}$, [**13**]$^+$; and $\mathrm{CFc_2^+}$, [**14**]$^+$. Most new compounds have been characterised by elemental analyses, and all by spectroscopy. Their spectra are consistent with their formulae; of particular interest is the UV–Vis spectrum of [**14**]$^+$ which shows two very strong absorption bands at 389 and 835 nm. X-ray diffraction techniques were used to determine the structures of **1** (R = Me), **4**, **6**, [**7**]Cl, **8**, **9**, **10**, **11a** (*syn* isomer), and **12**. All have the same basic structure with the Co atom sandwiched between ca. planar $\eta^5\text{-}\mathrm{C_5H_4R}$ and $\eta^4\text{-}\mathrm{C_4Ph_4}$ rings. The Ph groups do not lie in the $\mathrm{C_4}$ planes, and the $\mathrm{C_4Ph_4}$ ligands constitute four-bladed propellers. The two rings are close to parallel with interplanar angles of 0.4–4.4° except where R = CH(Fc)OH (6.6°) and $\mathrm{CFc_2OH}$ (12°) which is attributed to steric crowding though this does not affect the ferrocenyl groups to the same extent. When the C atom α to the $\mathrm{C_5H_4}$ ligand is $\mathrm{sp^3}$ hybridised, it is usually displaced out of the $\mathrm{C_5}$ plane away from Co, but when $\mathrm{C_\alpha}$ is $\mathrm{sp^2}$ hybridised (in **8** and **10**) it is displaced out of the $\mathrm{C_5}$ plane towards Co. This is attributed to the contribution that η^6-fulvene mesomers make towards a description of the structure of the latter compounds but not the former. In the primary and secondary alcohols **4** and **12** there is H-O···H-O hydrogen bonding, but in the tertiary alcohol **9** there is evidence of an intramolecular Fe···HO bond to one ferrocenyl group Fe···H = 2.965(1) Å and an angle of 5.1° between its two cyclopentadienyl ligands. Electrochemical studies are reported for **8**–**11** and the known compound triferrocenylcarbinol; this last is compared with the mixed cobalt/ferrocenyl systems **8** and, particularly, **9**. The $\mathrm{Co}(\eta^4\text{-}\mathrm{C_4Ph_4})(\eta^5\text{-}\mathrm{C_5H_4\text{-}})$ centre is always more difficult to oxidise than $\mathrm{Fe}(\eta^5\text{-}\mathrm{C_5H_5})(\eta^5\text{-}\mathrm{C_5H_4\text{-}})$.

1. Introduction

It is fifty years since $[\mathrm{Co}(\eta^4\text{-}\mathrm{C_4Ph_4})(\eta^5\text{-}\mathrm{C_5H_5})]$ was first reported by Nakamura and Hagihara [1], and there are now over four hundred papers and patents relating to (cyclobutadiene)(cyclopentadienyl) cobalt derivatives. A lot of recent work has been application driven, with several different foci: asymmetric synthesis and catalysis [2], molecular rotors [3] and as a Tamoxifen analogue [4]. The chemistry of $[\mathrm{Co}(\eta^4\text{-}\mathrm{C_4Ph_4})(\eta^5\text{-}\mathrm{C_5H_5})]$ complexes however is not as well-developed as that of the ferrocenyl analogues. One reason for this is that, compared with ferrocene, $[\mathrm{Co}(\eta^4\text{-}\mathrm{C_4Ph_4})(\eta^5\text{-}\mathrm{C_5H_5})]$ is less susceptible to attack by many electrophiles. For example, although it reacts with mercuric acetate/perchloric acid and then lithium chloride to give $[\mathrm{Co}(\eta^4\text{-}\mathrm{C_4Ph_4})(\eta^5\text{-}\mathrm{C_5H_4HgCl})]$ in good yields, this is a reagent and product that are probably best avoided if possible; its Vilsmeier formylation with $\mathrm{POCl_3/HC(O)N(Me)Ph}$ gives a disappointing 8% yield of the more desirable $[\mathrm{Co}(\eta^4\text{-}\mathrm{C_4Ph_4})(\eta^5\text{-}\mathrm{C_5H_4CHO})]$ [5].

$[\mathrm{Co}(\eta^4\text{-}\mathrm{C_4Ph_4})(\eta^5\text{-}\mathrm{C_5H_4CHO})]$ and $[\mathrm{Co}(\eta^4\text{-}\mathrm{C_4Ph_4})(\eta^5\text{-}\mathrm{C_5H_4CO_2Me})]$ are readily prepared from $\mathrm{Na[C_5H_4R]}$, $\mathrm{[Co(PPh_3)_3Cl]}$ and then $\mathrm{Ph_2C_2}$ ($\mathrm{R = CHO}$ and $\mathrm{CO_2Me}$) [6–9], and we have found them to be effective entry compounds. Here they are used in a variety of reactions to prepare a diverse range of $[\mathrm{Co}(\eta^4\text{-}\mathrm{C_4Ph_4})(\eta^5\text{-}\mathrm{C_5H_4R})]$ complexes, some of which have been foreshadowed in our study of $[\mathrm{Co}(\eta^4\text{-}\mathrm{C_4R_4})(\eta^5\text{-}\mathrm{C_5H_4R})]$ (R = Me and Et) derivatives [10]. They include donor–π-acceptor systems, and mixed cobalt/ferrocene alcohols $[\mathrm{Co}(\eta^4\text{-}\mathrm{C_4Ph_4})\{\eta^5\text{-}\mathrm{C_5H_4CH}_n(\mathrm{Fc})_{2-n}\mathrm{OH}\}]$ (Fc = ferrocenyl; $n = 0, 1$). These alcohols are readily dehydroxylated to the di- and triarylmethyl

---

[*] Corresponding author. Tel.: +64 3 479 4897; fax: +64 3 479 7906.
E-mail address: mcadamj@alkali.otago.ac.nz (C.J. McAdam).

0022-328X/$ – see front matter © 2010 Elsevier B.V. All rights reserved.
doi:10.1016/j.jorganchem.2010.12.026

cation analogues $[Co(\eta^4\text{-}C_4Ph_4)(\eta^5\text{-}C_5H_4CHFc)]^+$ and $[Co(\eta^4\text{-}C_4Ph_4)(\eta^5\text{-}C_5H_4CFc_2)]^+$ isolated as their $[BF_4]^-$ salts. The cations are the counterparts of the previously reported $[Co(\eta^4\text{-}C_4Ph_4)(\eta^5\text{-}C_5H_4CHR)]^+$ (R = Bu^t and Ph) and $[Co(\eta^4\text{-}C_4Ph_4)(\eta^5\text{-}C_5H_4CPh_2)]^+$ [11,12].

Additionally, this work has resulted in two versatile new synthons, the Wittig and Horner–Wadsworth–Emmons reagents $[Co(\eta^4\text{-}C_4Ph_4)(\eta^5\text{-}C_5H_4CH_2PPh_3)]Cl$ and $[Co(\eta^4\text{-}C_4Ph_4)\{\eta^5\text{-}C_5H_4CH_2P(O)(OEt)_2\}]$ respectively. These provide access to organometallic functionalised alkenes, a research area currently attracting much attention [13]. This work will be covered in a subsequent paper [14].

2. Experimental

2 and **3** were prepared as reported previously [8], and the same procedure was used to prepare **1** [15]. A procedure for the synthesis of **4** has been published [9] since our original synthetic work; our similar methodology offers similar yield but reduced reaction time and is available in the Electronic Supplementary Information.

Tributyltin-ferrocene was prepared according to the literature [16]. TMEDA was dried from *n*-BuLi and then distilled under reduced pressure [17]. All other reagents were purchased from commercial sources unless otherwise stated. Column chromatography was performed on alumina (activity II or III) or silica (Merck 7734). All reactions were carried out under an atmosphere of nitrogen. IR spectra were recorded on a Perkin Elmer Paragon 1000 FTIR spectrometer having a resolution of 4 cm^{-1}. NMR spectra were recorded on Varian Inova 300, 400 or 500 MHz spectrometers. ^1H (300 and 400 MHz) and ^{13}C (75 and 100 MHz) chemical shifts are reported downfield from tetramethylsilane as the internal standard; ^{31}P (121 MHz) from H_3PO_4. All coupling constants are given in Hz. UV/Visible spectra were recorded on a UNICAM UV2 spectrometer. Elemental analyses were carried out in the Microanalytical Laboratory, University College Dublin.

Cyclic voltammetric experiments were carried out at 20 °C in CH_2Cl_2 solutions degassed with nitrogen. A three-electrode cell was used with Cypress Systems 1 mm diameter Pt or 1.4 mm glassy carbon working, Ag/AgCl reference and platinum wire auxiliary electrodes. Solutions were $\sim 10^{-3}$ M in electroactive material and contained 0.1 M $[Bu_4N][PF_6]$ as the supporting electrolyte. Voltammograms were recorded using a Powerlab/4sp computer-controlled potentiostat. All potentials are referenced to the reversible formal potential (taken as $E^0 = 0.00$ V) for the $[Fe(\eta^5\text{-}C_5Me_5)_2]^{+/0}$ process [18] where E^0 was calculated from the average of the oxidation and reduction peak potentials under conditions of cyclic voltammetry. Under the same conditions, E^0 calculated for $[Fe(\eta^5\text{-}C_5H_5)_2]^{+/0}$ was 0.55 V.

2.1. Synthesis of $[Co(\eta^4\text{-}C_4Ph_4)(\eta^5\text{-}C_5H_4CH_2Cl)]$, 5

Thionyl chloride (0.21 g, 3.44 mmol) was added dropwise over one hour to a cooled solution (0 °C) of **4** (0.82 g, 1.6 mmol) and pyridine (0.27 g, 3.44 mmol) in toluene (50 ml). The mixture was allowed to return to room temperature, stirred overnight and then filtered through a glass frit to remove the precipitate. The mixture was evaporated to dryness under a vacuum. The residue was recrystallised from a dichloromethane–pentane solution to give **5** as a yellow powder (yield 0.70 g, 85%). M.p. (dec) 160–162 °C. Found: C 76.95, H 4.85, Cl 6.25; $C_{34}H_{26}ClCo$ requires C 77.20, H 4.95, Cl 6.70%. IR υ/cm^{-1}: υ(C=C) 1597, 1498 (CH_2Cl_2); υ(C=C) 1595, 1497; υ(C–Cl) 819 (KBr). ^1H NMR ($CDCl_3$): δ 7.46–7.19 (m, 20H, Ph), 4.71 and 4.62 (t, $^3J_{H,H}$ 2 Hz, 2H, C_5H_4), 3.94 (s, 2H, CH_2). ^{13}C NMR ($CDCl_3$): δ 135.8, 128.8, 128.2 and 126.6 (C_4Ph_4), 93.2 (C_{ipso}, C_5H_4), 84.8 and 83.2 (CH, C_5H_4), 75.5 (C_4Ph_4), 42.0 (CH_2).

2.2. Synthesis of $[Co(\eta^4\text{-}C_4Ph_4)\{\eta^5\text{-}C_5H_4CH_2P(O)(OEt)_2\}]$, 6

Diethyl phosphite (0.21 ml, 1.57 mmol) and excess sodium (0.2 g) in toluene (30 ml) was stirred at 0 °C for 30 min, refluxed for 90 min, and cooled. The excess sodium solidified to a single ball and was removed manually. **4** (0.40 g, 0.78 mmol) was added to the refluxing reaction mixture in small portions over 10 min and reflux maintained for 4 h. The mixture was cooled, and quenched with a 20% w/v solution of sodium bicarbonate. After 20 min the organic layer was separated, washed with water, dried over $MgSO_4$, filtered, concentrated, and chromatographed (silica). Dichloromethane eluted unreacted **4** and THF-dichloromethane (1/19) eluted the product **6**. This crystallised as a brown solid from a dichloromethane–pentane solution (yield 0.24 g, 49%). M.p. 156–158 °C. Found: C 71.93, H 5.73, P 4.74, Co 9.58; $C_{38}H_{36}O_3PCo$ requires C 72.38, H 5.75, P 4.91, Co 9.35%. IR υ/cm^{-1}: υ(C=C) 1598, 1497 (CH_2Cl_2); υ(C=C) 1596, 1498, υ(P=O) 1248 (KBr). ^1H NMR ($CDCl_3$): δ 7.34–7.11 (m, 20H, Ph), 4.52 and 4.50 (m, 2H, C_5H_4), 3.81 (dq, $^3J_{H,P}$ 7 Hz, $^3J_{H,H}$ 7 Hz, 4H, CH_2CH_3), 2.14 (d, $^2J_{H,P}$ 19 Hz, 2H, $C_5H_4CH_2$), 1.09 (t, $^3J_{H,H}$ 7 Hz, 6H, CH_2CH_3). ^{13}C NMR ($CDCl_3$): δ 136.1, 128.8, 128.1, 126.3 (C_4Ph_4), 88.7 (C_{ipso}, C_5H_4), 83.9 and 83.5 (CH, C_5H_4), 75.0 (C_4Ph_4), 62.0 (d, $^2J_{C,P}$ 6 Hz, CH_2CH_3), 24.6 (d, $^2J_{C,P}$ 138 Hz, $C_5H_4CH_2$), 16.4 (CH_2CH_3).

2.3. Preparation of $[Co(\eta^4\text{-}C_4Ph_4)(\eta^5\text{-}C_5H_4CH_2PPh_3)]Cl$, [7]Cl

A mixture of triphenylphosphine (3.17 g, 12.1 mmol) and **5** (0.640 g, 1.21 mmol) in dry toluene (60 ml) was refluxed overnight, cooled, and filtered. The precipitate was washed with toluene and pentane, and recrystallised from chloroform-pentane solution to give yellow crystals of [**7**]Cl (yield 0.72 g, 75%). M.p. 262–265 °C. Found: C 78.65, H 5.18, Cl 4.80; $C_{52}H_{41}PClCo$ requires C 78.93, H 5.22, Cl 4.48%. IR υ/cm^{-1}: υ(C=C) 1597, 1497 (CH_2Cl_2); υ(C=C) 1595, 1498 (KBr). ^1H NMR ($CDCl_3$): δ 7.80–7.25 (m, 35H, Ph), 4.67 and 4.33 (m, 2H, C_5H_4), 3.48 (d, $^2J_{H,P}$ 12 Hz, 2H, CH_2). ^{31}P NMR ($CDCl_3$): δ 20.4. ^{13}C NMR ($CDCl_3$): δ 135.7 (d, $^4J_{C,P}$ 3 Hz, C_{para}, PPh_3), 135.2, 128.9, 128.6 and 127.0 (C_4Ph_4), 133.8 (d, $^2J_{C,P}$ 10 Hz, C_{ortho}, PPh_3), 130.5 (d, $^3J_{C,P}$ 12 Hz, C_{meta}, PPh_3), 117.3 (d, $^1J_{C,P}$ 86 Hz, C_{ipso}, PPh_3), 85.7 (d, $^3J_{C,P}$ 3 Hz, CH, C_5H_4), 84.7 (CH, C_5H_4), 82.9 (d, $^2J_{C,P}$ 2 Hz, C_{ipso}, C_5H_4), 76.4 (C_4Ph_4), 25.7 (d, $^1J_{C,P}$ 50 Hz, CH_2).

2.4. Preparation of $[Co(\eta^4\text{-}C_4Ph_4)\{\eta^5\text{-}C_5H_4C(O)Fc\}]$, 8, and $[Co(\eta^4\text{-}C_4Ph_4)(\eta^5\text{-}C_5H_4CFc_2OH)]$, 9 {$Fc = Fe(\eta^5\text{-}C_5H_5)(\eta^5\text{-}C_5H_4\text{-})$}

The addition of n-BuLi (0.81 ml, 1.3 mmol) to a solution of $[Fe(\eta^5\text{-}C_5H_5)(\eta^5\text{-}C_5H_4SnBu^n{}_3)]$ (0.78 g, 1.63 mmol) in dry THF (30 ml) at −78 °C gave an orange solution and precipitate of LiFc [16]. After 30 min, to this was added a solution of **2** (0.35 g, 0.65 mmol) in THF (5 ml). The mixture turned red and was stirred overnight. It was quenched with water (2 × 10 ml), and extracted with CH_2Cl_2. The organic layer was dried over magnesium sulphate, evaporated to dryness at reduced pressure, and the residue chromatographed on alumina (pentane–toluene; 1/1). The tertiary alcohol **9** eluted as the second band and the ketone **8** as the third. Both products were isolated and crystallised from dichloromethane–pentane solutions to give red-brown **8** (yield 0.087 g, 20%) and yellow-brown **9** (yield 0.074 g, 13%).

2.4.1. $[Co(\eta^4\text{-}C_4Ph_4)\{\eta^5\text{-}C_5H_4C(O)Fc\}]$, 8

M.p. 175–178 °C. Found: C 75.82, H 4.78, Co 8.13, Fe 7.92; $C_{44}H_{33}OFeCo$ requires C 76.31, H 4.80, Co 8.51, Fe 8.06%. IR υ/cm^{-1}: υ(C=O) 1625, υ(C=C) 1596, 1499, 1455 (CH_2Cl_2); υ(C=O) 1618, υ(C=C) 1605, 1499 (KBr). ^1H NMR ($CDCl_3$): δ 7.60–7.25 (m, 20H, Ph) 5.54 and 4.94 (t, $^3J_{H,H}$ 2 Hz, 2H, C_5H_4Co), 4.62 and 4.39 (t, $^3J_{H,H}$ 2 Hz, 2H, C_5H_4Fe), 4.19 (s, 5H, C_5H_5). ^{13}C NMR ($CDCl_3$): δ 194.3 (CO), 135.5, 129.2, 128.4 and 127.0 (C_4Ph_4), 95.4 (C_{ipso}, C_5H_4Co), 87.0 and 84.5

Table 1
Crystal data for (a) **1**, **4**, **6**, [**7**]Cl and **8** and (b) **9**, **10**, both forms of **11a** and **12**.

Compound	**1**	**4**	**6**	[**7**]Cl.2H_2O.$CHCl_3$	**8**
Empirical formula	$C_{34}H_{27}Co$	$C_{34}H_{27}OCo$	$C_{38}H_{36}O_3PCo$	$C_{53}H_{46}O_2PCl_4Co$	$C_{44}H_{33}OCoFe$
Formula weight	494.49	510.49	630.57	946.60	692.48
Temperature	293(2) K	293(2) K	100(2) K	100(2) K	100(2) K
Wavelength	0.71073 Å	0.71073 Å	0.71073 Å	0.71073 Å	0.71073 Å
Crystal system	Orthorhombic	Monoclinic	Triclinic	Monoclinic	Triclinic
Space group	Pbcn	Cc	P – 1	C2/c	P – 1
Unit cell dimensions	a = 20.9888(17) Å b = 14.8096(12) Å c = 32.301(3) Å α = 90° β = 90° γ = 90°	a = 20.976(2) Å b = 28.010(3) Å c = 9.3932(9) Å α = 90° β = 108.036(2)° γ = 90°	a = 10.6221(9) Å b = 17.4465(14) Å c = 17.9525(15) Å α = 75.414(2)° β = 75.766(1)° γ = 85.727(2)°	a = 24.5903(8) Å b = 12.5321(4) Å c = 30.0100(10) Å α = 90° β = 100.6070(10)° γ = 90°	a = 11.3276(7) Å b = 11.4871(7) Å c = 12.3527(8) Å α = 82.521(1)° β = 77.025(1)° γ = 87.221(1)°
Volume	10 040.2(14) Å^3	5247.6(9) Å^3	3120.6(4) Å^3	9090.1(5) Å^3	1552.68(17) Å^3
Z	16	8	4	8	2
Density (calculated)	1.309 Mg/m^3	1.292 Mg/m^3	1.342 Mg/m^3	1.383 Mg/m^3	1.481 Mg/m^3
Absorption coefficient	0.704 mm^{-1}	0.678 mm^{-1}	0.638 mm^{-1}	0.690 mm^{-1}	1.038 mm^{-1}
F(000)	4128	2128	1320	3920	716
Crystal size (mm)	0.20 × 0.10 × 0.05	1.20 × 0.20 × 0.15	0.50 × 0.40 × 0.20	0.60 × 0.50 × 0.50	0.20 × 0.10 × 0.05
θ range for data collection	1.80–24.00°	2.04–25.00°	1.90–26.00°	1.83–33.00°	1.70–27.00°
Index ranges	− 24 <= h <= 23, − 16 <= k <= 16, − 36 <= l <= 36	− 24 <= h <= 24, − 33 <= k <= 33, − 11 <= l <= 11	− 13 <= h <= 13, − 21 <= k <= 21, − 22 <= l <= 22	− 37 <= h <= 37, − 19 <= k <= 19, − 45 <= l <= 45	− 14 <= h <= 14, − 14 <= k <= 14, − 15 <= l <= 15
Reflections collected	63 258	37 310	50 562	81 147	25 805
Independent reflections	7880 [R(int) = 0.0468]	9200 [R(int) = 0.0396]	12 234 [R(int) = 0.0324]	16 884 [R(int) = 0.0210]	6769 [R(int) = 0.0338]
Completeness to θ = 24.0°	99.9%	99.9%	99.7%	98.5%	99.7%
Absorption correction	Semi-empirical from equivalents	Semi-empirical from equivalents	Semi-empirical from equivalents	Semi-empirical from equivalents	Semi-empirical from equivalents
Max. and min. transmission	0.9656 and 0.8255	0.9051 and 0.7186	0.8830 and 0.7513	0.7243 and 0.6406	0.9499 and 0.8284
Refinement method	Full-matrix least-squares on F^2	Full-matrix least-squares on F^2	Full-matrix least-squares on F^2	Full-matrix least-squares on F^2	Full-matrix least-squares on F^2
Data/restraints/parameters	7880/0/623	9200/2/651	12 234/0/1019	16 884/6/589[a]	6769/0/556
Goodness-of-fit on F^2	1.019	1.043	1.064	1.041	1.046
Final R indices [I > 2sigma(I)]	R1 = 0.0351, wR2 = 0.0792	R1 = 0.0387, wR2 = 0.0833	R1 = 0.0432, wR2 = 0.1144	R1 = 0.0391, wR2 = 0.0995	R1 = 0.0353, wR2 = 0.0878
R indices (all data)	R1 = 0.0483, wR2 = 0.0853	R1 = 0.0489, wR2 = 0.0878	R1 = 0.0504, wR2 = 0.1217	R1 = 0.0449, wR2 = 0.1034	R1 = 0.0443, wR2 = 0.0942
Largest diff. peak and hole	0.590 and −0.344 e Å^{-3}	0.420 and −0.176 e Å^{-3}	0.806 and −0.390 e Å^{-3}	1.132 and −1.139 e Å^{-3}	0.526 and −0.233 e Å^{-3}

Compound	**9.CH_2Cl_2**	**10**	**11a.CH_2Cl_2**	**11a.½$CHCl_3$**	**12**
Empirical formula	$C_{55}H_{45}OCl_2Fe_2Co$	$C_{37}H_{25}N_2Co$	$C_{41}H_{31}N_4O_4Cl_2Co$	$C_{81}H_{59}N_8O_8Cl_3Co_2$	$C_{44}H_{35}OCoFe$
Formula weight	963.44	556.52	773.53	1496.57	694.50
Temperature	100(2) K	150(2) K	100(2) K	100(2) K	293(2) K
Wavelength	0.71073 Å	0.71073 Å	0.71073 Å	0.71073 Å	0.71073 Å
Crystal system	Triclinic	Monoclinic	Monoclinic	Triclinic	Triclinic
Space group	P – 1	P2$_1$/c	P2$_1$/n	P – 1	P – 1
Unit cell dimensions	a = 10.570(3) Å b = 11.658(3) Å c = 18.863(7) Å α = 104.222(7)° β = 103.098(7)° γ = 95.925(5)°	a = 11.0164(10) Å b = 14.3726(13) Å c = 17.1720(16) Å α = 90° β = 98.0540(10)° γ = 90°	a = 15.7015(16) Å b = 11.1903(12) Å c = 20.930(2) Å α = 90° β = 109.596(2)° γ = 90°	a = 10.910(3) Å b = 10.987(3) Å c = 15.218(4) Å α = 107.282(4)° β = 98.832(5)° γ = 99.518(4)°	a = 11.487(8) Å b = 12.978(9) Å c = 13.216(10) Å α = 73.228(12)° β = 65.870(12)° γ = 67.095(13)°
Volume	2163.3(12) Å^3	2692.1(4) Å^3	3464.5(6) Å^3	1677.5(7) Å^3	1637(2) Å^3
Z	2	4	4	1	2
Density (calculated)	1.479 Mg/m^3	1.373 Mg/m^3	1.483 Mg/m^3	1.481 Mg/m^3	1.409 Mg/m^3
Absorption coefficient	1.205 mm^{-1}	0.667 mm^{-1}	0.700 mm^{-1}	0.682 mm^{-1}	0.985 mm^{-1}
F(000)	992	1152	1592	770	720
Crystal size (mm)	0.20 × 0.10 × 0.03	0.70 × 0.50 × 0.50	0.80 × 0.40 × 0.20	0.30 × 0.05 × 0.03	0.20 × 0.15 × 0.05
θ range for data collection	1.83–20.94°.	1.86–28.29°.	1.98–25.00°.	1.94–23.50°.	1.71–24.00°.
Index ranges	− 10 <= h <= 10, − 11 <= k <= 11, − 18 <= l <= 18	− 14 <= h <= 14, − 19 <= k <= 18, − 22 <= l <= 22	− 18 <= h <= 18, − 13 <= k <= 13, − 24 <= l <= 24	− 12 <= h <= 12, − 12 <= k <= 12, − 17 <= l <= 17	− 13 <= h <= 13, − 14 <= k <= 14, − 15 <= l <= 15
Reflections collected	8681	44 689	23 424	10 636	21 619
Independent reflections	4521 [R(int) = 0.0500]	6448 [R(int) = 0.0296]	6093 [R(int) = 0.0425]	4929 [R(int) = 0.0433]	5131 [R(int) = 0.0662]
Completeness to θ = 24.0°	97.9%	96.6%	99.9%	99.3%	100.0%
Absorption correction	Semi-empirical from equivalents	Numerical	Semi-empirical from equivalents	Semi-empirical from equivalents	Semi-empirical from equivalents
Max. and min. transmission	0.9647 and 0.4044	0.7314 and 0.6524	0.8726 and 0.6300	0.9798 and 0.6637	0.9524 and 0.8163
Refinement method	Full-matrix least-squares on F^2	Full-matrix least-squares on F^2	Full-matrix least-squares on F^2	Full-matrix least-squares on F^2	Full-matrix least-squares on F^2
Data/restraints/parameters	4521/0/551	6448/0/461	6093/0/473	4929/0/482	5131/0/436

Table 1 *(continued)*

Compound	**9**.CH_2Cl_2	**10**	**11a**.CH_2Cl_2	**11a**.½$CHCl_3$	**12**
Goodness-of-fit on F^2	1.002	1.039	1.055	1.079	1.163
Final R indices [I > 2sigma(I)]	R1 = 0.0481, wR2 = 0.1043	R1 = 0.0312, wR2 = 0.0796	R1 = 0.0513, wR2 = 0.1244	R1 = 0.0541, wR2 = 0.1144	R1 = 0.0633, wR2 = 0.1325
R indices (all data)	R1 = 0.0714, wR2 = 0.1118	R1 = 0.0359, wR2 = 0.0824	R1 = 0.0628, wR2 = 0.1308	R1 = 0.0707, wR2 = 0.1230	R1 = 0.0898, wR2 = 0.1423
Largest diff. peak and hole	0.590 and −0.506 e Å^{-3}	0.379 and −0.240 e Å^{-3}	0.922 and −0.613 e Å^{-3}	0.556 and −0.367 e Å^{-3}	0.436 and −0.424 e Å^{-3}

(*C*H, C_5H_4Co), 81.1 (C_{ipso}, C_5H_4Fe), 76.9 (C_4Ph_4) 71.3 and 70.9 (*C*H, C_5H_4Fe), 70.2 (C_5H_5). λ_{max}/nm (ε/dm^3 mol^{-1} cm^{-1}) (CH_2Cl_2): 279 (41 000); 335 (sh, 15 000); 385 (sh, 5700); 450 (sh, 2800).

2.4.2. *[Co(η^4-C$_4$Ph$_4$)(η^5-C$_5$H$_4$CFc$_2$OH)],* ***9***

M.p. 178–181 °C. Found: C 70.06, H 4.84, Co 5.98, Fe 11.43; $C_{54}H_{43}OCoFe_2.CH_2Cl_2$ requires C 68.56, H 4.71, Co 6.12, Fe 11.59%. IR υ/cm^{-1}: υ(C=C) 1594, 1499 (CH_2Cl_2); υ(OH) 3680, υ(C=C) 1594, 1498 (KBr). ^{1}H NMR ($CDCl_3$): δ 7.50–7.20 (m, 20H, Ph), 4.80, 4.40 (m, 2H, C_5H_4Co), 4.05 (s, 10H, C_5H_5Fe), 4.02, 3.96, 3.88, 3.32 (m, 2H, C_5H_4Fe), 2.34 {s, 1H, C(O*H*)}. ^{13}C NMR ($CDCl_3$): δ 136.9, 129.4, 128.3 and 126.6 (C_4Ph_4), 111.7 (C_{ipso}, C_5H_4Co), 99.6 (C_{ipso}, C_5H_4Fe), 83.2, 82.1 (*C*H, C_5H_4Co), 75.1 (C_4Ph_4), 72.6 {*C*(OH)}, 69.0 (C_5H_5), 68.2, 67.4, 67.2, 66.7 (*C*H, C_5H_4Fe). λ_{max}/nm (ε/dm^3 mol^{-1} cm^{-1}) (CH_2Cl_2): 294 (sh, 28 000); 384 (sh, 4000); 450 (sh, 2000).

2.5. *Preparation of [Co(η^4-C$_4$Ph$_4$){η^5-C$_5$H$_4$CH=C(CN)$_2$}],* ***10***

Two drops of triethylamine were added to a solution of malononitrile (0.02 g, 0.27 mmol) and **3** (0.10 g, 0.20 mmol) in dry dichloromethane (30 ml), and the mixture stirred overnight. When the solvent was removed at reduced pressure, it gave a deep red residue which was chromatographed on silica (dichloromethane–pentane; 1/1). Deep red crystals of **10** were grown from dichloromethane/pentane mixtures (yield 0.085 g, 77%). M.p. 203–204 °C. Found: C 79.61, H 4.55, N, 5.06; $C_{37}H_{25}N_2Co$ requires C 79.85, H 4.53, N 5.03%. IR υ/cm^{-1}: υ(C≡N) 2225, υ(C=C) 1577, 1499 (CH_2Cl_2); υ(C≡N) 2218, υ(C=C) 1569, 1498 (KBr). ^{1}H NMR ($CDCl_3$): δ 7.42–7.25 (m, 20H, Ph), 6.87 (s, 1H, C*H*=C(CN)$_2$), 5.35 and 5.07 (t, ^{3}J$_{H,H}$ 2 Hz, 2H, C_5H_4). ^{13}C NMR ($CDCl_3$): δ 157.4 (*C*H=C(CN)$_2$), 134.3, 128.9, 128.8 and 127.8 (C_4Ph_4), 114.9 and 114.2 (*C*N), 90.4 and 85.2 (*C*H, C_5H_4), 87.9 (C_{ipso}, C_5H_4), 78.9 (C_4Ph_4). λ_{max}/nm (ε/dm^3 mol^{-1} cm^{-1}) (CH_2Cl_2): 277 (35 000); 322 (sh, 16 000); 360 (sh, 8400); 421 (7700), 500 (sh, 3500).

2.6. *Preparation of syn and anti-[Co(η^4-C$_4$Ph$_4$){η^5-C$_5$H$_4$CH=NNHC$_6$H$_4$(NO$_2$)$_2$-2,4}],* ***11a*** *and* ***11b***

Molecular sieves (4 Å) were added to a solution of **3** (0.25 g, 0.49 mmol) and dried 2,4-dinitrophenylhydrazine (0.15 g, 0.74 mmol) in dry dichloromethane (50 ml), and the mixture refluxed overnight. It was allowed to cool, filtered and the filtrate concentrated. *Syn* and *anti* isomers of the product (**11a** and **11b** respectively) were separated by chromatography (silica; pentane–dichloromethane; 5/2) and each crystallised from dichloromethane/pentane mixtures to give red **11a** (yield 0.071 g, 21%) and **11b** (yield 0.094 g, 28%).

2.6.1. *Syn-[Co(η^4-C$_4$Ph$_4$){η^5-C$_5$H$_4$CH=NNHC$_6$H$_4$(NO$_2$)$_2$-2,4}],* ***11a***

M.p. 228–230 °C. Found C 69.21, H 4.37, N 7.79, Co, 7.86; $C_{40}H_{29}O_4N_4Co$ requires C 69.77, H 4.24, N 8.14, Co 8.56%. IR υ/cm^{-1}: υ(C=N) 1616, υ(C=C) 1592, 1498, υ(NO_2) 1518, 1336 (CH_2Cl_2); υ(C=N) 1616, υ(C=C) 1593, 1495, υ(NO_2) 1514, 1331 (KBr). ^{1}H NMR ($CDCl_3$): δ 11.13 (s, 1H, N*H*), 9.06 {d, ^{4}J$_{H,H}$ 2 Hz, 1H, *H*$_3$, $C_6H_3(NO_2)_2$}, 8.28 {dd, ^{4}J$_{H,H}$ 3 Hz and ^{3}J$_{H,H}$ 10 Hz, 1H, *H*$_5$, $C_6H_3(NO_2)_2$}, 7.86 {d, ^{3}J$_{H,H}$ 10 Hz, 1H, *H*$_6$, $C_6H_3(NO_2)_2$}, 7.46–7.14 (m, 20H, Ph), 7.04 (s, 1H, C*H*=N), 5.29 and 4.93 (t, ^{3}J$_{H,H}$ 2 Hz, 2H, C_5H_4). ^{13}C NMR (75.4 MHz, $CDCl_3$): δ 145.3, 138.2 and 128.1 {*C*$_1$, *C*$_2$ and *C*$_4$ $C_6H_3(NO_2)_2$}, 143.3 (*C*H=N), 135.1, 128.9, 128.4 and 127.2 (C_4Ph_4), 129.9, 123.5 and 116.8 {*C*$_5$, *C*$_3$ and *C*$_6$, $C_6H_3(NO_2)_2$}, 88.4 and 83.6 (*C*H, C_5H_4), 85.9 (C_{ipso}, C_5H_4), 76.8 (C_4Ph_4). λ_{max}/nm (ε/dm^3 mol^{-1} cm^{-1}) (CH_2Cl_2): 270 (45 000); 315 (22 000); 386 (19 000).

2.6.2. *Anti-[Co(η^4-C$_4$Ph$_4$){η^5-C$_5$H$_4$CH=NNHC$_6$H$_4$(NO$_2$)$_2$-2,4}],* ***11b***

M.p. 177–178 °C. Found C 69.63, H 4.52, N 7.69, Co, 8.16; $C_{40}H_{29}O_4N_4Co$ requires C 69.77, H 4.24, N 8.14, Co 8.56%. IR υ/cm^{-1}: υ(C=N) 1615, υ(C=C) 1585, 1498, υ(NO_2) 1517, 1337 (CH_2Cl_2); υ(C=N) 1613, υ(C=C) 1583, 1495, υ(NO_2) 1512, 1333 (KBr). ^{1}H NMR (399.8 MHz, $CDCl_3$): δ 10.53 (s, 1H, N*H*), 9.14 {d, ^{4}J$_{H,H}$ 2 Hz, 1H, *H*$_3$, $C_6H_3(NO_2)_2$}, 8.32 {dd, ^{4}J$_{H,H}$ 3 Hz and ^{3}J$_{H,H}$ 10 Hz, 1H, *H*$_5$, $C_6H_3(NO_2)_2$}, 7.83 {d, ^{3}J$_{H,H}$ 10 Hz, 1H, *H*$_6$, $C_6H_3(NO_2)_2$}, 7.46–7.14 (m, 20H, Ph), 7.08 (s, 1H, C*H*=N), 5.10 and 4.91 (t, ^{3}J$_{H,H}$ 2 Hz, 2H, C_5H_4). ^{13}C NMR (125.7 MHz, $CDCl_3$): δ 145.9 (*C*H=N), 144.3, 137.8 and 128.3 {*C*$_1$, *C*$_2$ and *C*$_4$ $C_6H_3(NO_2)_2$}, 135.5, 129.0, 128.3 and 127.0 (C_4Ph_4), 130.0, 123.9 and 116.8 {*C*$_5$, *C*$_3$ and *C*$_6$, $C_6H_3(NO_2)_2$}, 89.5 (C_{ipso}, C_5H_4), 86.3 and 82.9 (*C*H, C_5H_4), 76.9 (C_4Ph_4). λ_{max}/nm (ε/dm^3 mol^{-1} cm^{-1}) (CH_2Cl_2): 259 (41 000); 315 (23 000); 414 (21 000).

2.7. *Preparation of [Co(η^4-C$_4$Ph$_4$){η^5-C$_5$H$_4$CH(Fc)OH}],* ***12*** *{Fc=Fe(η^5-C$_5$H$_5$)(η^5-C$_5$H$_4$-)}*

n-BuLi (0.32 ml, 0.5 mmol) and then TMEDA (0.08 ml, 0.5 mmol) were added dropwise to a cooled solution (0 °C) of ferrocene (0.112 g, 0.6 mmol) in dry diethyl ether, and the mixture stirred overnight [19]. This solution was cooled to −78 °C and a solution of **3** (0.100 g, 0.2 mmol) in THF (20 ml) added dropwise to it. The mixture was allowed to return to room temperature and stirred for a further 3 h. It was cooled to −78 °C, hydrolysed with water (10 ml), and extracted with dichloromethane. The dichloromethane solution was washed with brine, dried over magnesium sulphate, concentrated and chromatographed on silica (pentane–dichloromethane; 2/3). The product was crystallised from pentane–dichloromethane to give yellow-brown **12** (yield 0.040 g, 29%). Found: C 75.00, H 5.14, Co 8.02, Fe 7.70; $C_{44}H_{35}OCo\,Fe$ requires C 76.09, H 5.08, Co 8.49, Fe 8.04%. IR υ/cm^{-1}: υ(C=C) 1605, 1492 (CH_2Cl_2); υ(OH) 3671, υ(C=C) 1603, 1493 (KBr). ^{1}H NMR ($CDCl_3$): δ 7.50–7.24 (m, 20H, Ph), 4.92, 4.58, 4.56 and 4.53 (m, 1H, C_5H_4Co), 4.82 {d, ^{3}J$_{H,H}$ 3 Hz, 1H, C*H*(OH)}, 4.05, 4.02, 4.01 and 3.80 (m, 1H, C_5H_4Fe), 4.03 (s, 5H, C_5H_5), 1.64 {d, ^{3}J$_{H,H}$ 3 Hz, 1H, CH(O*H*)}. ^{13}C NMR ($CDCl_3$): δ 136.5, 129.0, 128.4 and 126.6 (C_4Ph_4), 103.4 (C_{ipso}, C_5H_4Co), 93.1 (C_{ipso}, C_5H_4Fe), 83.7, 82.4, 80.9, 80.9 (*C*H, C_5H_4Co), 75.1 (C_4Ph_4), 68.8 (C_5H_5), 67.9, 67.8, 67.1, 66.4 (*C*H, C_5H_4Fe), 66.7 {*C*H(OH)}.

2.8. *The reaction of [Co(η^4-C$_4$Ph$_4$){η^5-C$_5$H$_4$CH(Fc)OH}],* ***12****, with HBF$_4$.OEt$_2$. The formation of [Co(η^4-C$_4$Ph$_4$){η^5-C$_5$H$_4$CH(Fc)}][BF$_4$],* ***[13]****[BF$_4$] {Fc = Fe(η^5-C$_5$H$_5$)(η^5-C$_5$H$_4$-)}*

When two drops of $HBF_4.Et_2O$ were added to a solution of **12** in dichloromethane at room temperature, the colour changed from yellow to deep green/blue. The solution was washed with water (5 ml) to remove any excess acid, and the organic layer passed through a pad of pre-dried Celite. The eluant, a solution of [**13**][BF_4], was concentrated and analysed. ^{1}H NMR ($CDCl_3$): δ 8.09 (s, 1H, C*H*), 7.38–7.18 (m, 20H, Ph), 5.92, 5.73, 4.84 and 4.34 (m, 1H, C_5H_4Fe), 5.76, 5.35, 5.25 and 5.06 (m, 1H, C_5H_4Co), 4.65 (s, 5H, C_5H_5). ^{13}C NMR

(125.7 MHz, $CDCl_3$): δ 148.0 (*C*H, C_α), 133.3, 128.7, 128.6 and 127.9 (C_4*Ph*$_4$), 93.4 (*C*$_{ipso}$, C_5H_4Co), 90.6 (*C*$_{ipso}$, C_5H_4Fe), 94.9, 94.9, 90.0 and 80.9 (*C*H, C_5H_4Co), 87.9, 87.5, 80.8 and 73.4 (*C*H, C_5H_4Fe), 81.2 (*C*$_4Ph_4$), 78.5 (*C*$_5H_5$).

2.9. *The reaction of [Co(η^4-C_4Ph_4)(η^5-$C_5H_4CFc_2OH$)],* ***9****, with $HBF_4.OEt_2$. The formation of [Co(η^4-C_4Ph_4)(η^5-$C_5H_4CFc_2$)][BF_4], [****14****][BF_4], {Fc = Fe(η^5-C_5H_5)(η^5-C_5H_4-)}*

When two drops of $HBF_4.Et_2O$ or aqueous HBF_4 were added to a solution of **9** in dichloromethane at room temperature, the colour changed from yellow-brown to deep green/blue. The solution was washed with water (5 ml) to remove any excess acid, and the organic layer passed through a pad of pre-dried Celite. The eluant, a solution of [**14**][BF_4], was evaporated to dryness and the residue analysed. The UV/Visible spectrum of this compound was obtained by carrying out this reaction in a suitable cell. Found: C 58.77, H 4.06, Co 5.57, Fe 9.49; $C_{54}H_{42}$ $BF_4CoFe_2.(CH_2Cl_2)_2.H_2O$ requires C 59.20, H 4.26, Co 5.19, Fe 9.83%. ^{1}H NMR ($CDCl_3$): δ 7.40–7.20 (m, 20H, Ph), 5.83 (s, br, 2H, C_5*H*$_4$) 5.36 (s, br, 6H, C_5*H*$_4$), 5.16 (s, br, 4H, C_5*H*$_4$), 4.38 (s, 10H C_5*H*$_5$). ^{13}C NMR (125.7 MHz, $CDCl_3$): δ 196.9 (C_α), 132.9, 128.4, 128.1 and 127.8 (C_4*Ph*$_4$), 102.7 (*C*$_{ipso}$, C_5H_4Co), 88.3 (*C*$_{ipso}$, C_5H_4Fe), 94.1 and 89.6 (*C*H, C_5H_4Co), 81.3 (*C*$_4Ph_4$), 80.5 and 78.8 (*C*H, C_5H_4Fe), 75.0 (*C*$_5H_5$). λ_{max}/nm (ε/dm^3 mol^{-1} cm^{-1}) (CH_2Cl_2): 389 (13 000); 555 (2600); 616 (2800); 835 (7700).

2.10. *[{Fe(η^5-C_5H_5)(η^5-C_5H_4)}$_3$C][BF_4]*

The UV/Visible spectrum of this compound was obtained by adding a drop of aqueous HBF_4 to a solution of [{Fe(η^5-C_5H_5)(η^5-C_5H_4-)}$_3$COH] in dichloromethane in a suitable cell. Work-up of this solution as per [**14**][BF_4] afforded a sample for electrochemical studies. λ_{max}/nm (ε/dm^3 mol^{-1} cm^{-1}) (CH_2Cl_2): 395 (24 000); 585 (sh, 900); 855 (12 000).

2.11. *Crystal structure determinations*

The structures of **1**, **4**, **6**, [**7**]Cl, **8**, **9**, **10**, **11a**, and **12** were determined by X-ray crystallography in the X-ray laboratory of University College Dublin. Crystals were grown by slow diffusion and evaporation methods using $CDCl_3$–pentane, CH_2Cl_2–pentane and toluene–pentane mixtures. Data were collected on a Bruker SMART Apex CCD diffractometer. Semi-empirical absorption corrections based on redundant reflections were made using SADABS [20]. The structures were solved by direct methods using SHELXS-97 and refined by full-matrix least-squares on F^2 using SHELXL-97 [21]. All non-hydrogen atoms were assigned anisotropic temperature factors. For compounds **1**, **4**, [**7**]Cl, **9**, **11a** and **12** all hydrogen atoms were added at calculated positions and refined using a riding model. Their isotropic temperature factors were fixed to 1.2 times (1.5 times for methyl groups) the equivalent isotropic displacement parameters of the carbon/nitrogen atom to which the H atom is attached. For compounds **6**, **8** and **10** all hydrogen atoms were located in the difference Fourier map and allowed to refine freely with isotropic temperature factors. For [**7**]Cl, the O–H distances in the water molecules of crystallization were restrained to 0.9 Å. ORTEX [22] and Mercury [23] were used to calculate some interplane angles and interatomic separations.

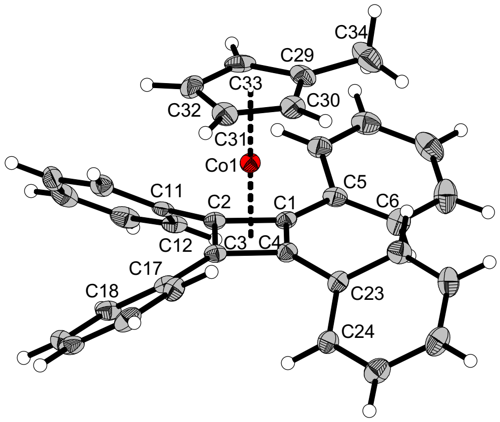

Fig. 1. Molecular structure and atom labeling of [Co(η^4-C_4Ph_4)(η^5-C_5H_4Me)], **1** (molecule 1 illustrated). Selected bond lengths (Å) C29–C34 1.501(4); Co–C_4Ph_4(cent) 1.689(1), Co–C_5H_4(cent) 1.669(1). Selected bond angles (°) C_5H_4(cent)–Co–C_4Ph_4(cent) 179.22 (2); C_4–C_5(Co) (interplane angle between C_4 and C_5 ligands on Co) 0.5.

Crystal data for **1**, **4**, **6**, [**7**]Cl, **8**, **9**, **10**, both types of **11a** and **12** are given in Table 1. Their molecular structures and atom labeling are shown in Figs. 1–9 which also include some selected molecular dimensions.

3. Results and discussion

The reactions carried out in the course of this work are summarized in Schemes 1 and 2. All compounds **1**–**12** are air-stable solids soluble in the appropriate solvents. Most are yellow to red-brown except where the groups R = CH=C(CN)$_2$ (**10**) and CH=$NNHC_6H_3(NO_2)_2$-2,4 (**11**) which are deep red. The merocyanine [**13**][BF_4] and $[CPh_3]^+$ analogue [**14**][BF_4] are deep blue–green.

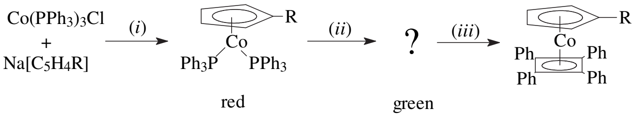

Scheme 1. (*i*) Tetrahy2drofuran solution, 20 °C. (*ii*) Add 2 equivalents of C_2Ph_2 in toluene, 20 °C. (*iii*) Reflux for 16 h.

[Co(η^4-C_4Ph_4)(η^5-C_5H_5)] is efficiently prepared in a single pot as shown in Scheme 1 from [Co$(PPh_3)_3$Cl] and Na[C_5H_5] via red [Co(η^5-C_5H_5)$(PPh_3)_2$] which reacts with two equivalents of Ph_2C_2 to give a green unidentified intermediate which is converted on heating to yellow-brown [Co(η^4-C_4Ph_4)(η^5-C_5H_5)] [11]. However, unlike ferrocene, this does not undergo facile electrophilic substitution reactions at the cyclopentadienyl ligand and is not, in general, a suitable precursor for other [Co(η^4-C_4Ph_4)(η^5-C_5H_4R)] complexes. It has been shown that these are best prepared by the same route as [Co(η^4-C_4Ph_4)(η^5-C_5H_5)] but with Na[C_5H_4R] salts in step 1, and proceeding to the desired complex utilising conventional organic chemistry to modify R as necessary [7–9,11]. However, yields of [Co(η^4-C_4Ph_4)(η^5-C_5H_4R)] vary considerably as a function of R and although both **2** and **3** are desirable entry compounds, the yield of **2** (R = CO_2Me) at 67% is greater than that of **3** (R = CHO) at 16%. **3** can be prepared from **2** in much higher yields (60% based on [Co$(PPh_3)_3$Cl]) by reduction to the primary alcohol **4** (Scheme 2) and subsequent oxidation to **3** [9,24].

In the current work we converted the primary alcohol **4** to the chloromethyl complex **5** by reaction with thionyl chloride and pyridine. We had hoped to prepare the bromo-analogue of **5** directly from **1** by reaction with N-bromosuccinimide and dibenzoylperoxide or azobisisobutyronitrile (AIBN), but both reactions failed. **5** proved an excellent precursor for the triphenyl phosphonium salt [**7**]Cl, but it failed to react with $P(OEt)_3$. The Horner–Wadsworth–Emmons reagent **6** [25] was obtained in the same way as its ferrocene counterpart [26] by a modification of the basic Michaelis reaction [27] in which Na[P(O)$(OEt)_2$] is reacted with the alcohol **4**.

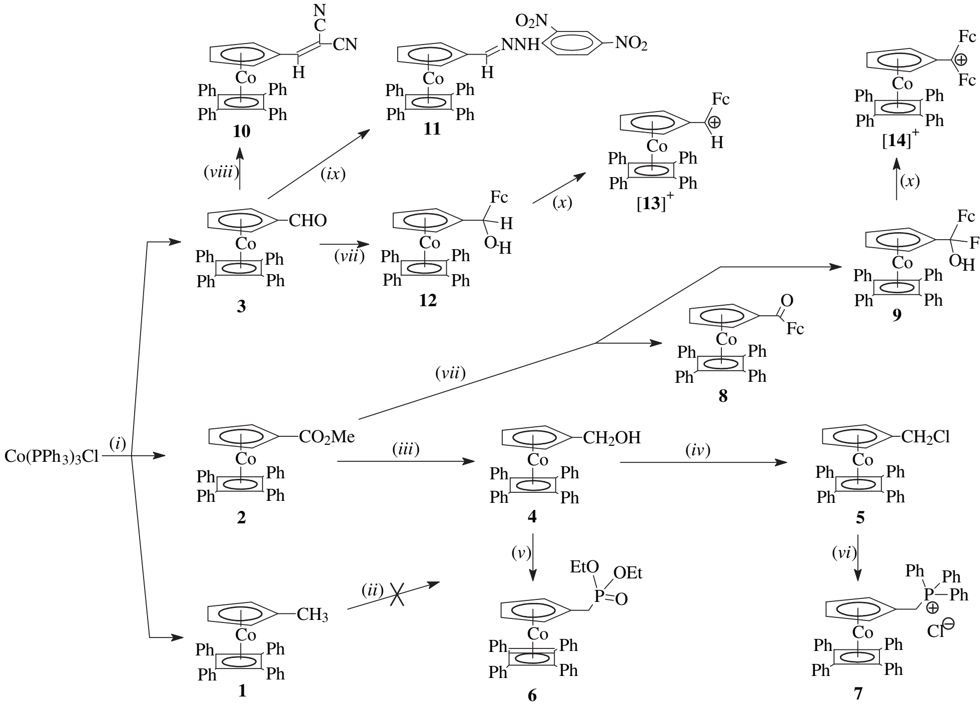

Scheme 2. (*i*) See Scheme 1. (*ii*) N-bromosuccinimide (NBS)/PhCOO$_2$COPh/hv or NBS/AIBN. (*iii*) LiAlH$_4$/Et$_2$O. (*iv*) SOCl$_2$/pyridine. (*v*) Na[P(O)(OEt)$_2$/toluene/Δ. (*vi*) Ph$_3$P/toluene/Δ. (*vii*) LiFc/THF. (*viii*) CH$_2$(CN)$_2$/Et$_3$N. (*ix*) 2,4-C$_6$H$_3$(NO$_2$)$_2$NHNH$_2$. (*x*) HBF$_4$.OEt$_2$/CH$_2$Cl$_2$.

The reaction of **2** with Li[Fe(η^5-C$_5$H$_5$)(η^5-C$_5$H$_4$)], LiFc, gives two products, the mixed ketone **8**, [Co(η^4-C$_4$Ph$_4$){η^5-C$_5$H$_4$C(O)Fc}], and the tertiary alcohol **9**, [Co(η^4-C$_4$Ph$_4$){η^5-C$_5$H$_4$CFc$_2$OH}]. The [Co(η^4-C$_4$Ph$_4$){η^5-C$_5$H$_4$CPh$_2$OH}] counterpart of **9** was prepared by the reaction of [Co(η^4-C$_4$Ph$_4$)(η^5-C$_5$H$_4$Li)] with Ph$_2$CO [8,9]. **8** has been previously prepared in lower yield by a Friedel-Crafts type reaction of [Co(η^4-C$_4$Ph$_4$){η^5-C$_5$H$_4$C(O)}]$^+$ with ferrocene [28].

The aldehyde **3** undergoes many conventional reactions such as the base-promoted Knoevenagel condensation with CH$_2$(CN)$_2$/Et$_3$N [29] which gives the dicyanoethene derivative **10**, and the condensation reaction with 2,4-dinitrophenylhydrazine to give the hydrazone **11** as separable *syn* and *anti* isomers **11a** and **11b** respectively. It also reacts with LiFc to give the secondary alcohol **12**, [Co(η^4-C$_4$Ph$_4$){η^5-C$_5$H$_4$CH(Fc)OH}]; we have previously reported similar reactions of **3** with LiR (R = ^{t}Bu and Ph) which give the secondary alcohols [Co(η^4-C$_4$Ph$_4$){η^5-C$_5$H$_4$CH(R)OH}] [11].

Both the secondary alcohol **12** and the tertiary alcohol **9** react with HBF$_4$.OEt$_2$ to give very intensely coloured green-blue products which, on the basis of their spectra are judged to be respectively the merocyanine salt [Co(η^4-C$_4$Ph$_4$)(η^5-C$_5$H$_4$CHFc)][BF$_4$], [**13**][BF$_4$], and the triarylmethyl cation counterpart, [Co(η^4-C$_4$Ph$_4$)(η^5-C$_5$H$_4$CFc$_2$)][BF$_4$], [**14**][BF$_4$], similar to the [Co(η^4-C$_4$Ph$_4$)(η^5-C$_5$H$_4$CHR)][BF$_4$] and [Co(η^4-C$_4$Ph$_4$)(η^5-C$_5$H$_4$CPh$_2$)][BF$_4$] salts previously described [11,12]. Although these are reasonably stable compounds, they did not afford crystals suitable for X-ray diffraction.

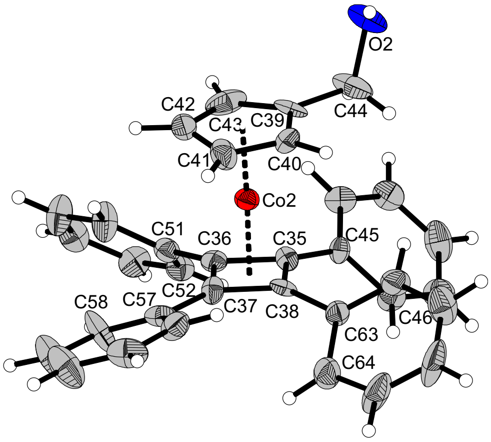

Fig. 2. Molecular structure and atom labeling of [Co(η^4-C$_4$Ph$_4$)(η^5-C$_5$H$_4$CH$_2$OH)], **4** (molecule 2 illustrated). Selected bond lengths (molecules 1/2, Å) Co–C$_4$Ph$_4$(cent) 1.692(1)/1.684(1); Co–C$_5$H$_4$(cent) 1.674(1)/1.667 (1); C33–C34/C67–C68 1.522(6)/1.471(5); C34–O1/C68–O2 1.377(6)/1.429(4); O2-H2O…O1#1 1.85; O1-H1O…O2#2 1.80. Selected bond angles (molecules 1/2, °) C34–O1–H10/C68–O2–H2O 109.5/109.5; C$_5$H$_4$(cent)–Co–C$_4$Ph$_4$(cent) 178.66(2)/176.65(3); C$_4$–C$_5$(Co) 0.4/3.1.

3.1. Spectroscopy

The most important bands in the IR spectra of **5**–**12** are those due to the vibrations of the phenyl groups of the η^4-C$_4$Ph$_4$ ligands, especially the υ(C=C) modes which give rise to two strong absorption bands at ca. 1498 and 1595 cm^{-1}. There are few differences between them except where an IR-active ancillary group R is present. Thus its υ(CO) vibrations give rise to a strong absorption bands in the spectrum of the ferrocenyl ketone **8** (1625 cm^{-1}). This frequency is comparable to that reported for the analogous ferrocene derivative diferrocenyl ketone (1612 cm^{-1} [30]) and is shifted to higher energy relative to [Co(η^4-C$_4$Ph$_4$){η^5-C$_5$H$_4$C(O)CH$_3$}] (1672 cm^{-1}) [11] and ferrocenecarboxaldehyde (1690 cm^{-1} [31]). The υ(CN) vibrations of the dicyanoethene **10** give rise to a strong absorption band at 2220 cm^{-1} which is higher than the 2185/2170 cm^{-1} pair observed for its ferrocenyl counterpart [32] but both are lower than that of CH$_2$(CN)$_2$, 2274 cm^{-1} [33]. The absorption bands at ca. 1616 cm^{-1} in the IR spectra of the hydrazones **11a** and **11b** are assigned to their υ(C=N) vibrations, but also present are bands at ca.1336 and 1518 cm^{-1} due to their υ(NO$_2$) vibrations, frequencies close to those observed for C$_6$H$_5$NO$_2$ (1347 and 1521 cm^{-1}) [34]. There is a strong

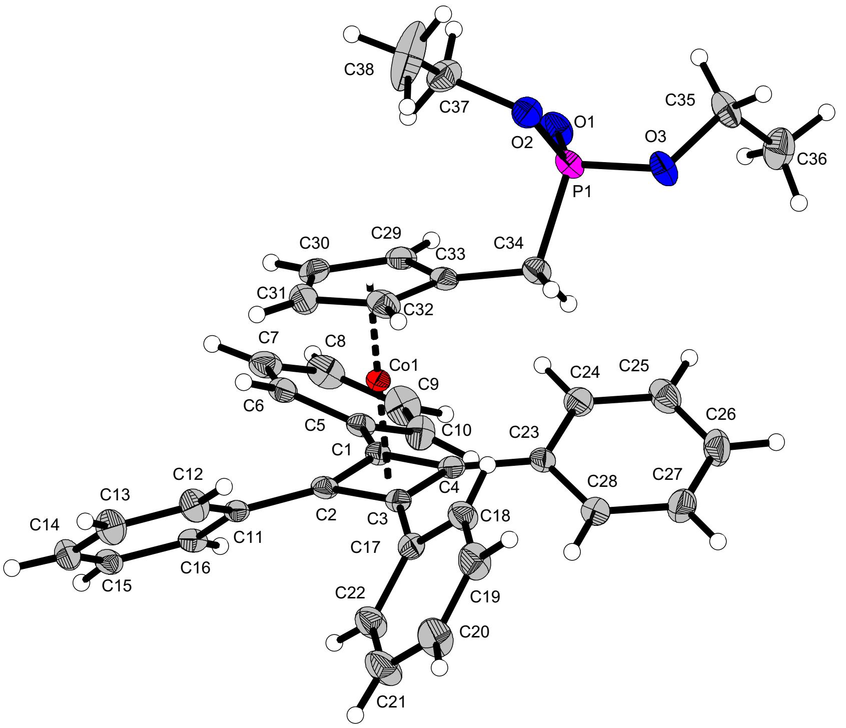

Fig. 3. Molecular structure and atom labeling of $[Co(\eta^4\text{-}C_4Ph_4)\{\eta^5\text{-}C_5H_4CH_2P(O)(OEt)_2\}]$, **6** (molecule 1 illustrated). Selected bond lengths (molecules 1/2, Å) Co–C_4Ph_4(cent) 1.682(1)/1.689(1); Co–C_5H_4(cent) 1.667(1)/1.671(1); C33–C34 1.501(3)/1.501(3); C34–P(1) 1.794(2)/1.795(2); P(1)–O(1) 1.4638(16)/1.4643(16); P(1)–O(2) 1.5820(16)/1.5727(16); P(1)–O(3) 1.5759(16)/1.5799(15). Selected bond angles (molecules 1/2, °) C32–C33–C34 126.4(2)/126.8(2); C29–C33–C34 126.0(2)/125.6(2); C33–C34–P1 110.74(15)/113.04(15); O1–P1–C34 114.78(10)/114.11(10); O3–P1–C34 101.70(10)/106.22(10); O2–P1–C34 106.65(10)/104.73(9); C_5H_4(cent)–Co–C_4Ph_4(cent) 176.62(2)/178.29(2); C_4–C_5(Co) 4.4/2.4.

absorption band at 819 cm^{-1} in the spectrum of the chloromethyl complex **5** which is assigned to its υ(C–Cl) vibration, and one at 1248 cm^{-1} in the spectrum of the phosphonate which is assigned to its υ(P=O) mode. The υ(OH) vibrations of the primary alcohol **4**, the secondary alcohol **12** and the tertiary alcohol **9** give rise to weak though readily identified absorption bands in their spectra at 3401, 3671 and 3680 cm^{-1} respectively. The first of these is broad but the other two are sharp. This suggests that the OH group of **4** partakes of hydrogen bonding but those of **12** and **9** do not. Additional evidence for this comes from X-ray crystallographic studies, and is discussed in Section 3.2.

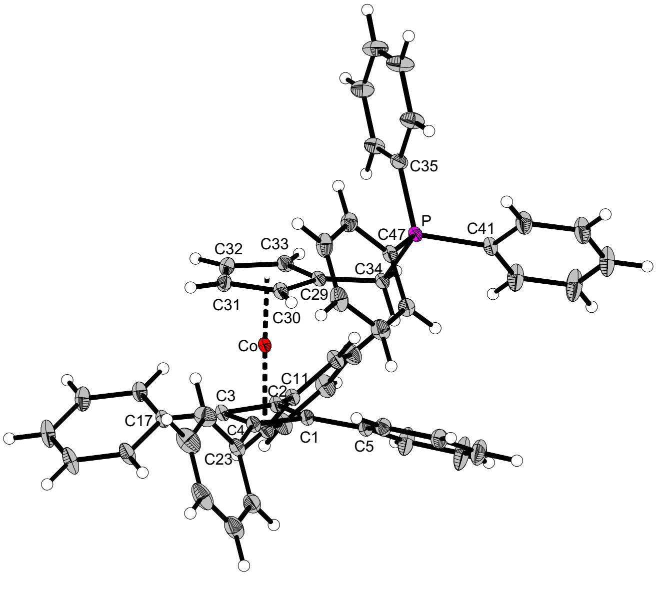

Fig. 4. Molecular structure and atom labeling of the cation of $[Co(\eta^4\text{-}C_4Ph_4)(\eta^5\text{-}C_5H_4CH_2PPh_3)]Cl.2H_2O.CHCl_3$, [**7**]$Cl.2H_2O.CHCl_3$. Selected bond lengths (Å) Co–C_4Ph_4(cent) 1.695(1); Co–C_5H_4(cent) 1.680(1); C29–C34 1.5032(15); C34–P 1.8111(11). Selected bond angles (°) C33–C29–C34 124.27(10); C30–C29–C34 128.05(10); C29–C34–P 113.88(7); C35–P–C34 112.03(5); C47–P–C34 107.43(5); C41–P–C34 108.27(5); C_5H_4(cent)–Co–C_4Ph_4(cent) 177.73(1); C_4–C_5(Co) 3.8.

The ^1H NMR spectra of **5**–**12** are consistent with their known or anticipated structures. The complex multiplet due to the twenty protons of the η^4-$C_4(C_6H_5)_4$ ligand are not greatly affected by R. The cyclopentadienyl protons of the η^5-C_5H_4R ligands where R is not chiral give rise to two triplets or unresolved broad resonances, each integrating for two protons. If R has inherent chirality as in **12**, all four Co(η^5-C_5H_4) protons are magnetically inequivalent and give rise to a distinctive set of four multiplets each integrating for a single proton. The introduction of ferrocenyl groups into R increases the number of cyclopentadienyl resonances. The singlet and two triplets due to the Fe(η^5-C_5H_5) and Fe(η^5-C_5H_4) are generally found upfield of their Co(η^5-C_5H_4) counterparts. As with the Co(η^5-C_5H_4) resonances, the chiral molecule **12**, shows four Fe(η^5-C_5H_4) multiplets. The Fe(η^5-C_5H_5) remains a singlet. The spectrum of **9** is unusual. Symmetry generated inequivalence about the C_α pyramid generates two Co(η^5-C_5H_4) and one Fe(η^5-C_5H_5) resonance, but four due to Fe(η^5-C_5H_4) as illustrated in Fig. 10.

Other ^1H NMR resonances for **5**–**12** show the anticipated chemical shifts and multiplicity associated with coupling to adjacent protons or, in the case of **6** and **7**, ^{31}P atoms. The spectra of **11a** and **11b** do not allow either to be defined, but the X-ray diffraction shows **11a** to be the *syn* isomer so **11b** is assumed to be the *anti*. The spectra for these compounds also feature very broad signals at δ 11.13 and 10.53 respectively. They disappear on treatment with D_2O and so are attributed to the N*H* protons. For most hydrazones, these are found at δ 7–8; here the downfield shift and the broadened signal suggest that the amine protons are engaged in hydrogen

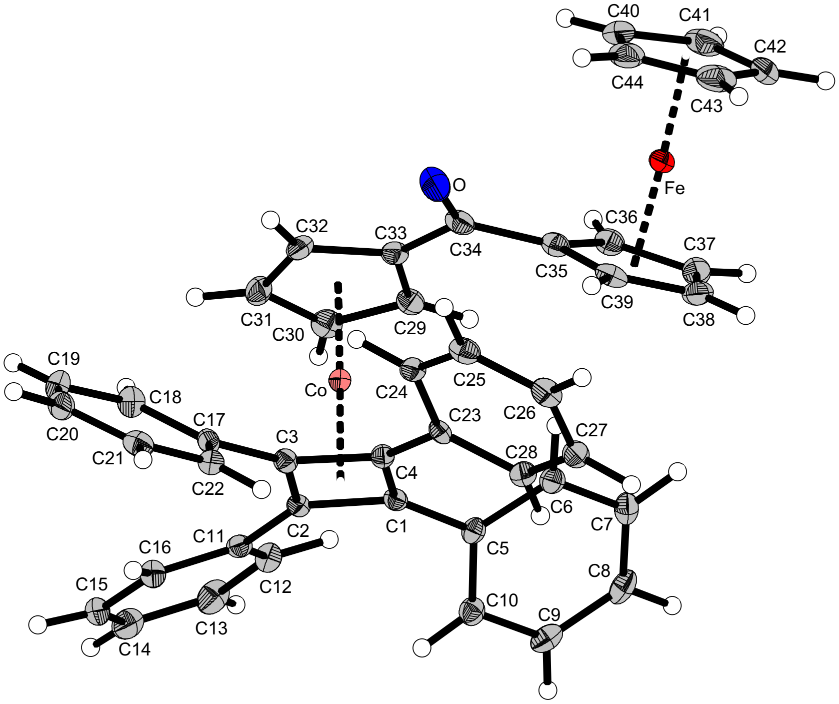

Fig. 5. Molecular structure and atom labeling of [Co(η^4-C_4Ph_4){η^5-$C_5H_4C(O)Fc$}], **8**. Selected bond lengths (Å) Co–C_4Ph_4(cent) 1.697(1); Co–C_5H_4(cent) 1.681(1); C33–C34 1.474(3); C34–C35 1.482(3); Fe–C_5H_4(cent) 1.648(1); Fe–C_5H_5(cent) 1.653(1). Selected bond angles (°) C33–C34–O1 120.23(19); C35–C34–O1 121.25(19); C_5H_4(cent)–Fe–C_5H_4(cent) 178.15 (2); C_5–C_5(Fe) 3.5(1); C_5H_4(cent)–Co–C_4Ph_4(cent) 177.10(2); C_4–C_5(Co) 3.5(2).

bonding with the oxygen of the *ortho*-positioned nitro groups as found in the solid state for **11a**.

The ^{13}C NMR spectra of **5**–**12** contain the expected η^4-C_4Ph_4 ligand signals, again largely independent of R. The Co(η^5-C_5H_4) ligands give rise to three resonances unless R is chiral when five are observed. Introduction of ferrocenyl groups leads the presence of further four resonances or six in a chiral molecule. These generally lie upfield of those due to Co(η^5-C_5H_4). In **9**, the Co(η^5-C_5H_4R) moiety gives rise to three resonances as expected but the Fe(η^5-C_5H_4R) groups give rise to five each for the reasons outlined above (Fig. 10). The resonances due to other groups in R are as expected with coupling to ^{31}P in both **6** ($^1J_{C,P} = 138$ Hz) and **7** ($^1J_{C,P} = 50$ Hz) as well as coupling to OEt and Ph groups respectively. In all solid state structures (see below) the C_4Ph_4 ligand acts as a four-bladed propeller and a source of molecular chirality. However, this chirality is not maintained in solution (see above) as the single ^{13}C NMR signals for both *o* and *m* C_6H_5 atoms confirms that rotations about the C-C_6H_5 and Co-C_4Ph_4/C_5H_4R axes are fast on the NMR timescale.

The UV/Visible spectra of most of **5**–**12** are very similar to that of [Co(η^4-C_4Ph_4)(η^5-C_5H_5)] which shows a very intense absorption band below 250 nm, a strong band at 274 nm and a very weak band at 412 nm [35]. Thus when the C_5H_4-C_α carbon atom is sp^3 hybridised, the observed spectrum is the summation of the [Co(η^4-C_4Ph_4)(η^5-C_5H_4–)] and –R parts e.g. in the alcohols **9** and **12** which contain ferrocenyl groups. However, when this carbon atom is sp^2 hybridised and R is a –CH=X group, the [Co(η^4-C_4Ph_4)(η^5-C_5H_4–)] moiety is part of a potential donor–π–acceptor system, extra or red-shifted absorption band appear in the electronic spectra and such compounds are a much darker red, e.g. **10**, {R = –CH=C(CN)$_2$} shows a strong absorption band at 421 nm and a shoulder at ca. 500 nm. The better electron donor properties of ferrocene are evident in the ferrocenylogue [Fc–CH=C(CN)$_2$] where the maxima are observed at longer wavelengths, 395 and 521 nm [32].

The salts [**13**][BF_4] and [**14**][BF_4] are formed when yellow solutions of the alcohols **12** and **9** are respectively treated with HBF_4.OEt_2 or aqueous HBF_4. They are an intense green-blue in colour. For the latter this is due to the presence of strong absorption bands in its UV/Visible spectra at 389 and 835 nm and much weaker ones at 555 and 616 nm which are not present in the spectrum of the alcohol **9**. The analogous triferrocenylmethyl cation [36] has a similar spectrum, but the strong bands are more intense and appear at longer wavelength at 395 and 855 nm, and the absorption in the visible region 550–620 nm is barely discernible.

However, it is their NMR spectra which give the most structural information about these salts. The cation formation is accompanied by a marked deshielding of many but not all ^{1}H resonances. Thus the (η^5-C_5H_4–)M protons of **12** which lie between δ 4.53–4.92 when M = Co and δ 3.80–4.05 when M = Fe, shift to δ 4.34–5.92 in the cation [**13**]$^+$ whilst the (η^5-C_5H_5)Fe signal shifts from δ 4.03 to 4.65. The most dramatic effect is noted for the exocyclic C_α-*H* resonance which moves from δ 4.82 to δ 8.09, whereas the $C_4(C_6H_5)_4$ protons are unaffected. Similar changes in chemical shifts are observed for the **9**/[**14**]$^+$ pair of δ 3.32–4.80 to δ 5.15–5.83 for the (η^5-C_5H_4), and δ 4.05 to δ 4.38 for (η^5-C_5H_5)Fe, whilst the $C_4(C_6H_5)_4$ protons are, again, unaffected.

The dehydroxylation of the alcohols has similar consequences for the ^{13}C NMR spectra. For each C atom there is a change of chemical shift $\Delta\delta = \delta_{cation} - \delta_{alcohol}$ which is generally positive as most become more deshielded on cation formation, but this is not universally the case. For the **12**/[**13**]$^+$ pair the largest Δδ (81.4 ppm) is for C_α; the others are much smaller with those for Co(η^5-C_4Ph_4) (η^5-C_5H_4–) < Fe(η^5-C_5H_5)(η^5-C_5H_4–). However, the Δδ for the *ipso* carbon atoms of both Co(η^5-C_5H_4–) and Fe(η^5-C_5H_4–) are negative i.e. the resonances of the cation lie upfield of those of the alcohol. This has been observed previously in the [Co(η^4-C_4Ph_4){η^5-$C_5H_4CH(OH)Ph$}]/[Co(η^4-C_4Ph_4)(η^5-C_5H_4CHPh)]$^+$ pair, where Δδ for C_{ipso} of Ph is negative though that for C_{ipso} of the Co(η^5-C_5H_4–) moiety is

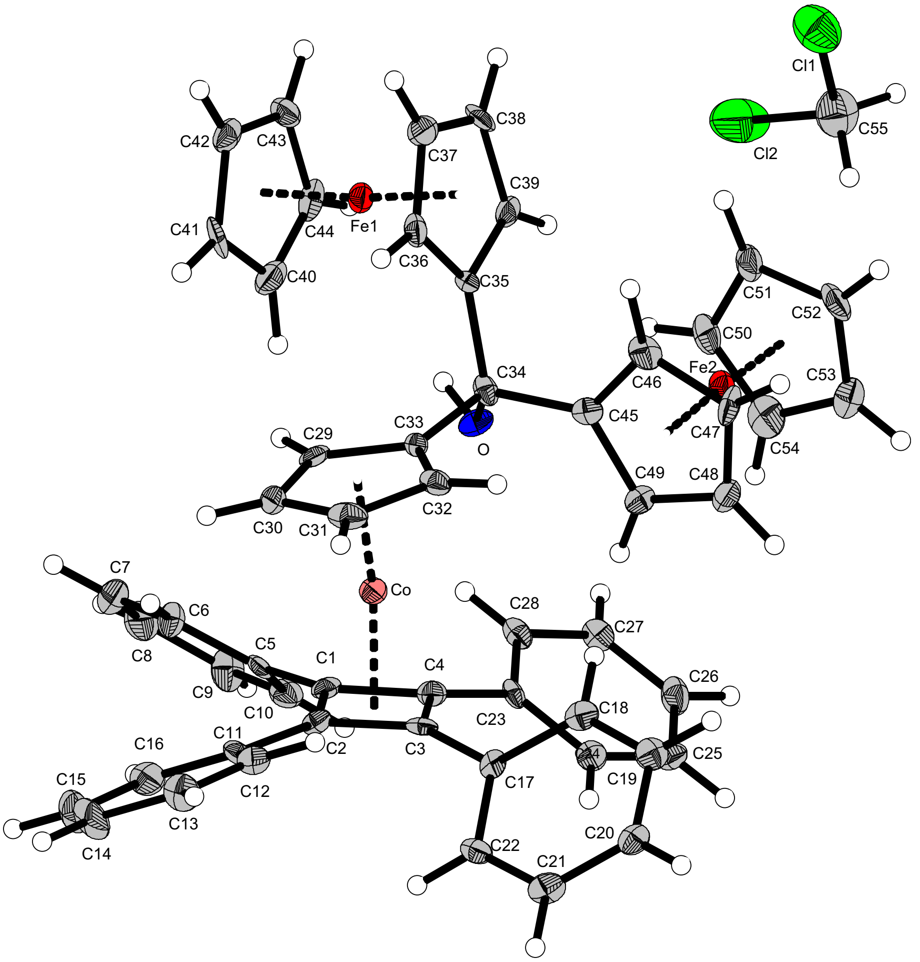

Fig. 6. Molecular structure and atom labeling of $[Co(\eta^4\text{-}C_4Ph_4)(\eta^5\text{-}C_5H_4CFc_2OH)].CH_2Cl_2$, **9**.$CH_2Cl_2$. Selected bond lengths (Å) Co–C_4Ph_4(cent) 1.707(7); Co–C_5H_4(cent) 1.682(6); C33–C34 1.530(8); C34–C35/C34–C45 1.524(8)/1.511(8). Selected bond angles (°) C33–C34–C35 110.4(4); C33–C34–C45 108.0(5); C35–C34–C45 109.4(4); Fe–(C_5H_4)(cent) 1.656(5)/1.647(4); Fe–C_5H_5(cent) 1.662(5)/1.648(4); C_5H_4(cent)–Fe–C_5H_4(cent) 175.82(6)/177.94(7); C_5–C_5(Fe) 5.1(5)/0; C_5H_4(cent)–Co–C_4Ph_4(cent) 172.23(5); C_4–C_5(Co) 11.9(4).

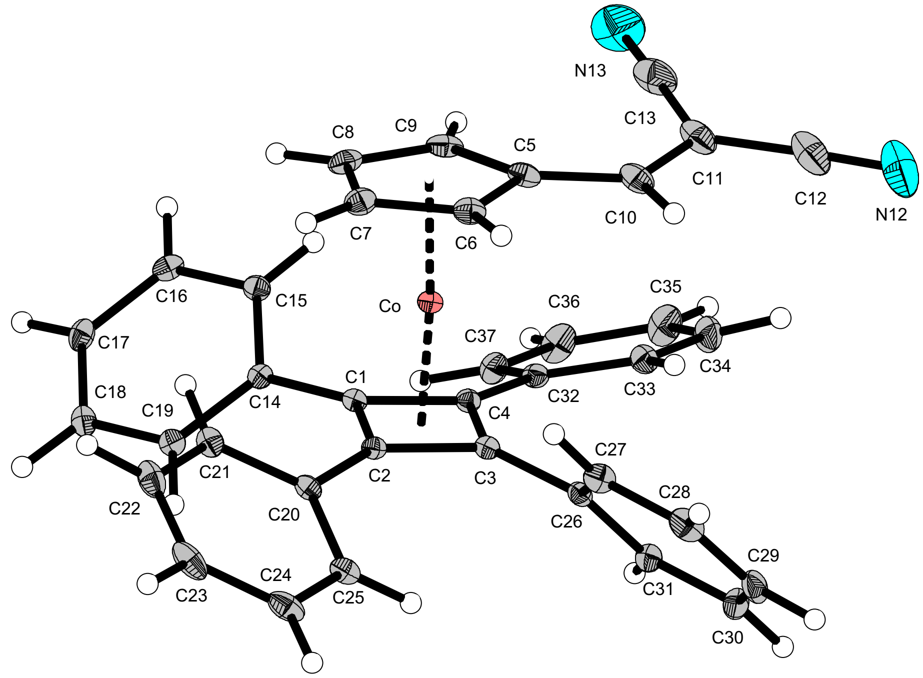

Fig. 7. Molecular structure and atom labeling of $[Co(\eta^4\text{-}C_4Ph_4)\{\eta^5\text{-}C_5H_4CH{=}C(CN)_2\}]$, **10**. Selected bond lengths (Å) Co–C_4Ph_4(cent) 1.693(1); Co–C_5H_4(cent) 1.677(1); C5–C10 1.432(2); C10–C11 1.356(2); C11–C12/C11–C13 1.356(2)/1.437(3). Selected bond angles (°) C10–C5–C6 122.90(13); C10–C5–C 130.32(14); C5–C10–C11 128.72(16); C10–C11–C12 119.43(17); C10–C11–C13 122.31(16); C_5H_4(cent)–Co–C_4Ph_4(cent) 175.4; C_4–C_5(Co) 4.4.

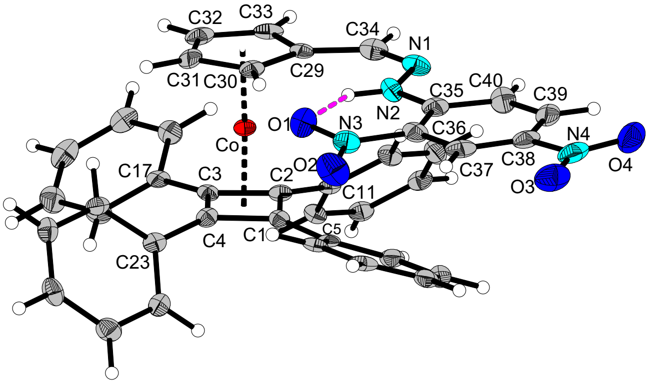

Fig. 8. Molecular structure and atom labeling of *syn*-[Co(η^4-C_4Ph_4){η^5-$C_5H_4CH{=}NNHC_6H_4(NO_2)_2$-2,4}], **11a**. Selected bond lengths (Å) for **11a**.CH_2Cl_2 {for **11a**.½$CHCl_3$} Co–C_4Ph_4(cent) 1.692(1) {1.692(3)}; Co–C_5H_4(cent) 1.679(1) {1.683(3)}; C29–C34 1.460(5) {1.455(5)}; C34–N1 1.296(5) {1.317(5)}; N1–N2 1.376(4) {1.383(4)}; N2–H2N…O1 1.95(4) {1.77(3)}. Selected bond angles (°) for **11a**.CH_2Cl_2 {for **11a**.½$CHCl_3$} C33–C29–C34 120.5(4) {119.3(3)}; C30–C29–C34 133.2(4) {106.5(3)}; C29–C34–N1 133.6(4) {134.2(3)}; C34–N1–N2 116.8(3) {114.3(3)}; C_5H_4(cent)–Co–C_4Ph_4(cent) 177.39(3) {179.20(3)}; C_4–C_5(Co) 1.2 {1.8}.

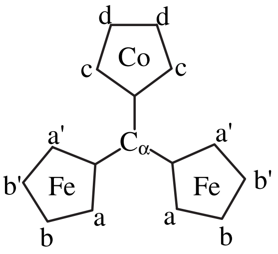

Fig. 10. The inequivalence of the (η^5-C_5H_4)Fe protons. A projection down the O–C_α axis of **9**, or the perpendicular to the trigonal plane of [**14**]$^+$.

positive Δδ [11]. We do not understand the reasons for this, but the general import of the spectral data is that the positive charge of the cation is delocalized from C_α into the adjacent Co(η^5-C_4Ph_4)(η^5-C_5H_4–) and Fe(η^5-C_5H_5)(η^5-C_5H_4–) substituents, and, given that $\Delta\delta_{Fe} > \Delta\delta_{Co}$, the ferrocenyl group is the more effective donor of the two. It is generally accepted that carbocations are stabilized by adjacent metal centres, and there is much evidence that in [(η^5-$C_5H_4C_\alpha HR$)Fe(η^5-C_5H_5)]$^+$ this happens by direct interaction of the metal atom with the C_α^+ (See the Introduction section of ref. [11]). The structure of [**13**]$^+$ may thus be represented by a hybrid of three mesomers, *I*, *II* and *III* (Fig. 11) with *II* predominating over *III*. These conclusions are consistent with work of Gleiter et al. who concluded that in [M(η-$C_5H_4CPh_2$)] systems the positive charge is more effectively delocalized on to the metal when M = Fe(η^5-C_5H_5) than when M = Co(η^4-C_4H_4) [37], and also with the oxidation potentials of the metallocenyl groups (see below).

When the alcohol **9** is converted to the cation [**14**]$^+$, the number of resonances due to the Fe(η^5-C_5H_4–) moieties declines from five to three and there is one due to the Fe(η^5-C_5H_5). Thus the *a*/*a*′ and *b*/*b*′ pairs of the two ferrocenyl groups in the cation are no longer in different NMR environments. This is a consequence of planar coordination about C_α in [**14**]$^+$ and rapid rotation about its C_α-C_{ipso} bonds. The chemical shift of the C_α resonance at δ 196.9 is much lower than that found in [**13**]$^+$ but its Δδ of 124.3 ppm is much larger and comparable to that observed for the Ph_3COH/Ph_3C^+ system (128 ppm) [38]. The Δδ for the (η^5-C_5H_4)Fe carbon atoms are larger than those for (η^5-C_5H_4)Co. However the Δδ for both these and (η^5-C_5H_5)Fe are smaller than those for the **12**/[**13**]$^+$ pair. The *ipso* C atoms for all three C_5H_4 groups show negative Δδ values. Taken as a whole this suggests that, as in [**13**]$^+$, the positive charge is delocalized away more effectively by the Fe centres than the Co, but because [**14**]$^+$ contains two ferrocenyl groups, the effect on each is less pronounced than on the single ferrocenyl group of [**13**]$^+$. When the structure of [**14**]$^+$ is represented by a resonance hybrid of four mesomers, each of the equivalents of *II* in Fig. 11 makes a smaller contribution than does *II* itself to [**13**]$^+$, and so the C_α-ferrocenyl bonds have a lower order in [**14**]$^+$ than in [**13**]$^+$.

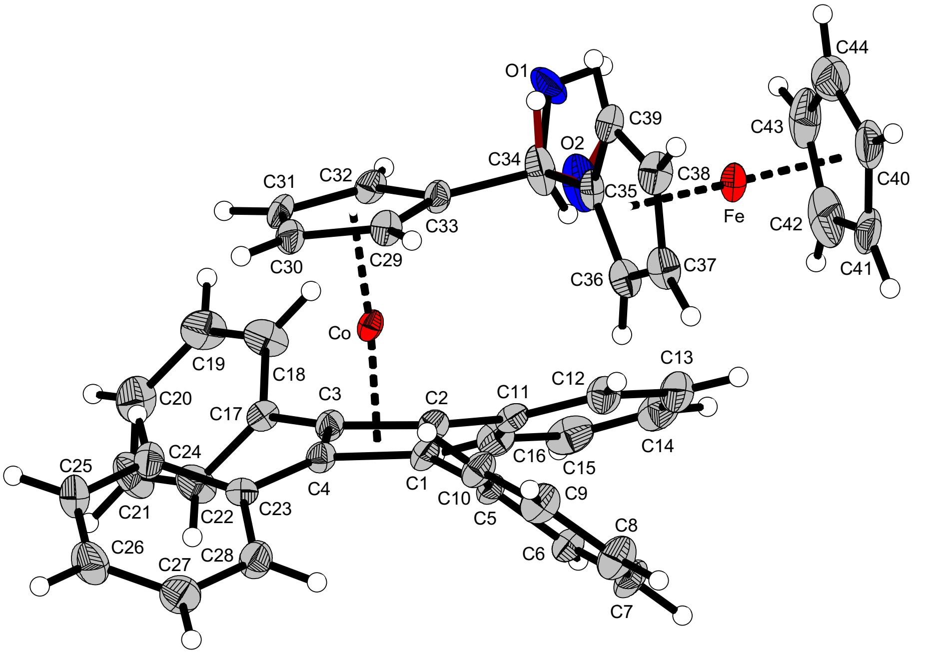

Fig. 9. Molecular structure and atom labeling of [Co(η^4-C_4Ph_4){η^5-$C_5H_4CH(Fc)OH$}], **12**. Selected bond lengths (Å) Co–C_4Ph_4(cent) 1.70(1); Co–C_5H_4(cent) 1.68(1); C33–C34 1.503 (8); C(34)–C(35) 1.497(8); Fe–C_5H_4(cent) 1.641(6); Fe–C_5H_5(cent) 1.641(6). Selected bond angles (°) C33–C34–O1/O2 109.8(6)/117(1); C35–C34–O1/O2 117.6(7)/120.6(8); C_5H_4(cent)–Fe–C_5H_4(cent) 177.06(9); C_5–C_5(Fe) 0; C_5H_4(cent)–Co–C_4Ph_4(cent) 174.92(6); C_4–C_5(Co) 6.6.

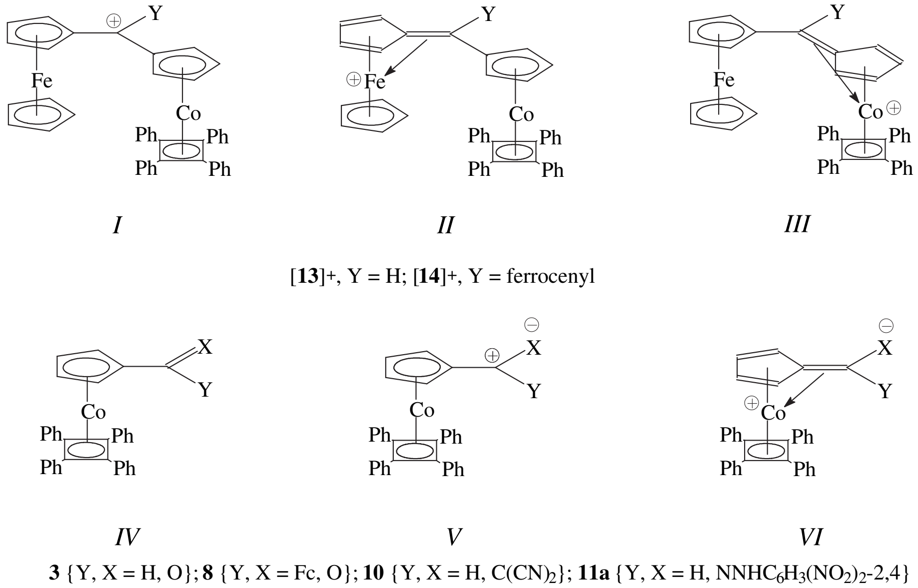

[**13**]+, Y = H; [**14**]+, Y = ferrocenyl

3 {Y, X = H, O}; **8** {Y, X = Fc, O}; **10** {Y, X = H, C(CN)$_2$}; **11a** {Y, X = H, NNHC$_6$H$_3$(NO$_2$)$_2$-2,4}

Fig. 11. Resonance forms of the [Co(η^4-C$_4$Ph$_4$)(η^5-C$_5$H$_4$CYFc)]$^+$ cations [**13**]$^+$ (Y = H) and [**14**]$^+$ (Y = Fc), and of various [Co(η^4-C$_4$Ph$_4$)(η^5-C$_5$H$_4$CY = X)] complexes.

3.2. Crystal structures

The crystal and molecular structures of **1**, **4**, **6**, [**7**]Cl, **8**, **9**, **10**, **11a** and **12** have been determined by X-ray diffraction techniques; that of **3** was reported previously [11]. They are shown in Figs. 1–9 together with the atom labeling. In the cases of **1**, **4** and **6** there are two molecules per asymmetric unit. Molecule 2 of **1** has disorder in the η^5-C$_5$H$_4$Me ring plane. The secondary alcohol **12** has H/OH disorder (55:45) at C$_\alpha$. The structure of **11a** was determined twice, once with crystals grown from CH$_2$Cl$_2$/pentane (structure 1) and the other with crystals grown from CHCl$_3$/pentane mixtures (structure 2); both define **11a** as the *syn* isomer and, hence, **11b** as the *anti* isomer.

All compounds adopt a sandwich structure with the Co atoms coordinated by planar η^5-C$_5$H$_4$R and η^4-C$_4$Ph$_4$ ligands. These rings are ca. parallel with angles of 0.4–4.4° between their planes except for **12** (6.6°) and **9** (12°). This distortion is probably a consequence of steric interactions between the η^4-C$_4$Ph$_4$ and CH(OH)Fc or C(OH)Fc$_2$ groups respectively. The relative orientations of the cyclopentadienyl and cyclobutadiene rings (Fig. 12) is configuration e in **1**, **3**, and **4** (molecule 1), b in **4** (molecule 2), b/e in **6**, (molecule 1), d in **6** (molecule 2), c/e in [**7**]$^+$, c in **8** and **9**, a in **10**, d in **11a** (structure 1), f in **11a** (structure 2) and **12**.

The phenyl groups of the η^4-C$_4$Ph$_4$ ligands do not lie in the C$_4$ plane. The C-C$_6$H$_5$ bonds point away from the Co atom atoms with centroid-C-C$_{Ph}$ angles of 169.0(4)–178.9(2)° (average = 173.8°). Furthermore, the phenyl rings are tilted with respect to the C$_4$ plane so that C$_4$Ph$_4$ constitutes a four-bladed propeller. The angles between the C$_4$ and C$_6$ planes are not the same in any one structure, though generally each of the *trans* pairs are tilted by comparable amounts. They lie between 19.0° and 66.5° with an average of 35.4°. Due to this synchronized tilting of the phenyl rings the molecules are inherently chiral and pack in the unit cells in symmetry generated *rac* pairs.

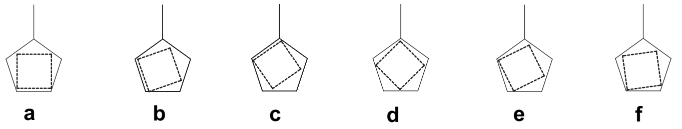

Fig. 12. Relative orientations of cyclobutadiene and cyclopentadienyl ligands in [Co(η^4-C$_4$Ph$_4$)(η^5-C$_5$H$_4$R)] complexes.

With the exception of **9**, and to a lesser extent **12**, normal bond lengths are observed for Co–C$_{Cb}$ (Cb = cyclobutadiene){1.968(2)–2.002(1) Å}, Co–C$_{Cp}$ {2.035(3)–2.098(1) Å}, C$_{Cb}$–C$_{Cb}$ {1.455(3)–1.479(5) Å}and C$_{Cp}$–C$_{Cp}$ {1.370(9)–1.457(8) Å}. For **9** the steric interactions which cause the anomalous angle between the Cp and Cb planes also bring about a lengthening of the Co bond to the *ipso* C$_5$H$_4$ atom, Co–C33 {2.116(6) Å} but not of Co–C29 or Co–C32 {2.068(5) and 2.095(5) Å} or of Co–C30 or C31 {2.032(5) and 2.050 (5) Å} whilst retaining the planarity of the C$_5$ ring. There is also a lengthening of the bond from Co to C4 of the C$_4$Ph$_4$ ligand {2.029 (5) Å} which is almost eclipsed by C33. Similar but far less significant effects are also observed for **12**.

8, **9** and **12** contain ferrocenyl (Fc) groups. Their ca. planar η^5-C$_5$ rings are close to parallel with interplanar angles varying from 1.8° in **12** to 5.1° for the Fc1 of **9**. They are almost exactly staggered in **8** (rotated by ca. 3.5° from the ideal), otherwise they are closer to eclipsed being rotated by 15° in **12** and by 6.2°/10° for Fc1/Fc2 in **9**. The Fe–C and C–C distances lie in the range 2.023(6)–2.062(2) Å (average 2.042 Å) and 1.389(9)–1.439(8) Å (av. 1.419 Å) for the C$_5$H$_4$ ligand, and 2.006(7)–2.062(2) Å (av. 2.041 Å) and 1.357(11)–1.449 (9) Å (av. 1.411 Å) for the C$_5$H$_5$ ligand. There is only limited distortion of the ferrocenyl groups in **9** and **12** (but see below) where the consequences of steric crowding are borne by the Co(η^4-C$_4$Ph$_4$)(η^5-C$_5$H$_4$) moiety.

In general, the bond lengths and angles within the R groups are normal. When the C$_\alpha$ of R is sp^3 hybridised, it generally lies close to the C$_5$H$_4$(Co) plane being displaced from it away from Co by between −0.024 and +0.057 Å, but in **12** the displacement is +0.104 Å and in **9** it is +0.158 Å away from Co, again probably due to steric effects. The projection along the C$_\alpha$–C$_{ipso}$(Co) bond shows that in most cases these molecules adopt one of the two conformations shown in Fig. 13 or close to them. **A** with X, Y = H is adopted by one molecule of **4**, both molecules of **6** and [**7**]$^+$, and **A** with Y = Fc by **12**. **9** is midway between A and B with Y = OH. One molecule of **4** and of **1** are closer to **B** than **A**, X, Y = H. Similarly for the ferrocenyl groups in **9** and **12**, C$_\alpha$ do not lie in the planes of the ferrocenyl C$_5$H$_4$ groups,

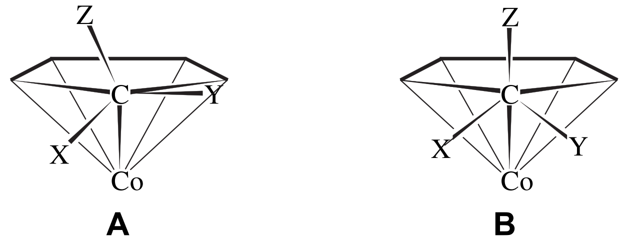

Fig. 13. Projection down the C_{ipso}–C_α axis of [Co(η^4-C_4Ph_4)(η^5-$C_5H_4C_\alpha$XYZ)] molecules.

but are displaced from them away from the metal atom by 0.07 Å in **12**, 0.11 Å for Fc1 in **9**, and 0.18 Å for Fc2 in **9**. The projection along the C_α–C_{ipso}(Fe) is close to **B** in **12** with Z = Co(η^4-C_4Ph_4)(η^5-C_5H_4–), whilst in **9** it is between **A** and **B** with Z = Fe2(η^5-C_5H_5)(η^5-C_5H_4–)/ Y = Co(η^4-C_4Ph_4)(η^5-C_5H_4–) for Fc1, and Z = Co(η^4-C_4Ph_4)(η^5-C_5H_4–)/Y = Fe1(η^5-C_5H_5)(η^5-C_5H_4–) for Fc2. As a consequence of the orientations adopted, the angles between the planes of the C_5H_4 ligands are all close to 90°; 86.7° in **12**, and 83°, 88° and 87.5° in **9** for Co/Fe1, Co/Fe2 and Fe1/Fe2 ligands respectively. A similar arrangement is found in [{Fe(η^5-C_5H_5)(η^5-C_5H_4-)}$_3$COH] where the ferrocenyl groups are close to eclipsed and the three Cp–Fe–Cp axes are essentially orthogonal to one another with C_5H_4 interplane angles of 95.4°, 90.9° and 92.7° [39].

When C_α is sp^2 hybridised in Co{η^5-C_5H_4C(Y) = X } systems it is normally displaced from the C_5H_4 plane by between −0.031 and 0.114 Å i.e. *towards* Co decreasing **3** (0.114 Å) > **8** (0.108 Å) > **10** (0.06 Å) > **11a** (−0.031 Å). This distortion may be a consequence of some Cα···Co interactions as in mesomer *VI* (Fig. 11). A similar series is also observed for the angle between the C_5H_4 and C_{ipso}–C(X)–Y planes which is 5.1° in the aldehyde **3**, 6.95° in the ketone **8**, 3.7 and 6.4° in the two structures of the hydrazone **11a** and 12.8° in the dicyanoethene **10**. Both of the series, but particularly the first, correlate with the decreasing electron-withdrawing nature of the C(Y)=X group C(H)=O > C(Fc)=O > C(H)=C(CN)$_2$ > C(H)=NNHC$_6$H$_3$(NO$_2$)$_2$, and the increasing importance of mesomer *IV* over mesomers *V* and *VI* in Fig. 11. For **8**, C_α lies 0.027 Å out of the C_5H_4(Fe) plane away from Fe, and the angle between this plane and the C–C(O)C– plane is 41.6°. This suggests that any C_α···Fe interaction is limited, and that the contribution that mesomers such as *III* (X = O$^-$) makes towards a description of the overall structure is not important. For **8**, the Fe(η^5-C_5H_5) moiety lies on the opposite side of the C–C_α(O)–C plane from Co (η^5-C_4Ph_4), and the angle between the two η^5-C_5H_4 planes is 45°.

There are a number of H-bonding interactions of note in these structures. In the primary alcohol **4** intermolecular···O2–H2···O1 –H1···O2–H2···O1–H1···interactions form molecular ribbons running through the lattice with H2···O1/H2···O1–H1 = 1.848(4) Å/ 174.5(2)° and H1···O2/H1···O2–H2 = 1.796(3) Å/167.7(3)°. In the secondary alcohol **12** the situation is more complicated. The diastereomer based on O2–H2 forms an H-bonded dimer with an adjacent O2- diastereomer though the H2···O2′ distances are much longer than in **4**, H2···O2′ = 2.305 Å and O2-H2···O2′ = 131.1°. The only other possible interactions are >3 Å. There are no similar interactions apparent in the structure of the tertiary alcohol **9**, but it does have an intramolecular Fe1···H1 separation of 2.965(1) Å with Fe1···H1-O1 = 127.2(2)°. The Fe1···H axis enters the ferrocenyl group between the C40–C44 and C35$_{ipso}$–C39 bonds though closer to the latter. Because the two C_5 rings are not parallel (dihedral angle 5.11°) it is at about this point that their separation is at its greatest with C35···C40 = 3.416(7) Å. By comparison C38···C43 = 3.219(6) Å whilst the Fe2(η^5-C_5H_4)(η^5-C_5H_5) moiety has near parallel rings (dihedral angle 2.3°) and an average C_{Cp}···C_{Cp} separation of 3.301 Å. It is tempting to regard the situation as the early stages of an electrophilic attack (protonation) on the Fe atom of a ferrocene. Intramolecular Fe···HO contacts are a common feature of 1-ferrocenyl alcohols [40,41]. For example in [Fe(η^5-C_5H_5){η^5-C_5H_4C(Ph)(Me)OH}] the two cyclopenatadienyl rings have a dihedral angle of 4.31° and Fe···H 2.94 (3) Å [40]. There are similar though weaker Fe···HO interactions in **12** (Fe···HO = 3.226(1) Å and Fe···H-O = 117.07° with a C_5H_4/C_5H_5 interplane angle of 1.8°) and [Fc$_3$COH] [39] (Fe1···HO = 3.2454(4) Å and Fe1···H-O = 115.4(2)°) with a C_5H_4/C_5H_5 interplane angle of 4.59°. Interplane angles for the Fe2 and Fe3 ferrocenyl components are 2.84 and 3.33° respectively. Here the Fe1···H axis enters the ferrocenyl group close to the C1$_{ipso}$–C6 (separation 3.406(4) Å) with the shortest interplanar contact between C4 and C9 = 3.218(5) Å.

11a shows an intramolecular hydrogen bond of NH with an O atom of the *o*-NO$_2$ group. In the **11a**.½CHCl$_3$ structure (2) this is relatively long with O1···H(2N) = 1.95(3) Å and O1···H-N2 = 130 (3)°, whereas in the **11a**.CH$_2$Cl$_2$ structure (1) it is shorter with O1···H(2N) = 1.77(3) Å and O1···H-N2 = 144(2)°.

3.3. Electrochemistry

Electrochemical data for **8**–**11** are given in Table 2 which also includes that for other compounds relevant to our discussion. In dichloromethane solution [Co(η^4-C_4Ph_4)(η^5-C_5H_5)] undergoes a chemically reversible oxidation at E^0 = 0.98 V (plus a second irreversible

Table 2
Electrochemical data[a] for **8**–**11**, [Fc$_3$COH] and various ferrocenyl derivatives for comparison.

	Compound[b]	Co(η^4-C_4Ph_4)(η^5-C_5H_4) oxidation		Fe(η^5-C_5H_5)(η^5-C_5H_4) oxidation
		E^0/V	i_{pc}/i_{pa}[c]	E^0/V
8	[Co(η^4-C_4Ph_4){η^5-C_5H_4C(O)Fc}]	1.22	0.6	0.72
9	[Co(η^4-C_4Ph_4){η^5-C_5H_4CFc$_2$(OH)}]	1.12	1.0	0.49, 0.69
10	[Co(η^4-C_4Ph_4){η^5-C_5H_4CH=C(CN)$_2$}]	1.25	0.3	
11a	*Syn*-[Co(η^4-C_4Ph_4)(η^5-C_5H_4CH=NNHC$_6$H$_4$(NO$_2$)$_2$-2,4})]	1.16	0.8	
11b	*Anti*-[Co(η^4-C_4Ph_4)(η^5-C_5H_4CH=NNHC$_6$H$_4$(NO$_2$)$_2$-2,4})]	1.08	0.7	
	[Fc$_3$COH]			0.47, 0.66, 0.76[d]
	[Co(η^4-C_4Ph_4)(η^5-C_5H_5)]	0.98	1.0	
	[Fe(η^5-C_5H_5)$_2$] [44]			0.55
	[Fc$_2$CO] [45],[e]			0.66, 0.85
	[PhFc$_2$COH] [45],[e]			0.45, 0.64

[a] 1×10^{-3} M in CH$_2$Cl$_2$/0.1 M [Bu$_4$N][PF$_6$]/100 mV s^{-1}/internal [Fe(η^5-C_5Me_5)$_2$]$^{0/+}$ reference.
[b] Fc = Fe(η^5-C_5H_5)(η^5-C_5H_4).
[c] i_{pc}/i_{pa} at 100 mV s^{-1}.
[d] E_m calculated from the average of the oxidation and reduction potentials.
[e] Converted from original SCE reference.

oxidation process at higher anodic potentials) [42,43]. [Co(η^4-C_4Ph_4)(η^5-C_5H_4R)], **8**–**11**, undergo a similar oxidation but at higher E^0, and it is only for **9** (R = CFc_2OH) that this is reversible. For other compounds it is quasi-reversible with the reverse to forward current ratio, $i_{pc}/i_{pa,}$ decreasing to 0.3 for **10**.

The ferrocenyl ketone **8** shows an additional wave associated with the fully chemically reversible $Fc^{+/0}$ couple ($i_{pc}/i_{pa} = 1.0$). Its E^0 of 0.72 V lies between the first and second oxidations reported for diferrocenyl ketone [45] (Table 2), consistent with the relatively poor electron donor ability of the Co(η^4-C_4Ph_4)(η^5-C_5H_4) fragment. Furthermore its peak-to-peak potential separation is about the same as that of the internal decamethylferrocene, $[Fe(\eta^5\text{-}C_5Me_5)_2]^{0/+}$, reference in this medium, which suggests that the wave can be considered Nernstian, the deviation from a 60 mV ΔE_p waveform being associated with uncompensated resistance as typically encountered in CH_2Cl_2 solution.

For **9**, two distinct chemically reversible ferrocenyl oxidations ($E^0 = 0.49$, 0.69 V; $\Delta E_{ox} = 200$ mV) are observed before the cobalt based oxidation at 1.12 V (Fig. 14). This suggests that the electronic communication between the two ferrocenyl groups is well defined despite the saturated link. Similar behaviour has been noted previously for $PhFc_2COH$ ($\Delta E_{ox} = 190$ mV), Fc_2CO and related polyferrocenyl compounds, and was attributed to a through-space mechanism [45,46].

We wished to compare the electrochemistry of **9** with that of its ferrocenyl counterpart triferrocenylcarbinol, [{Fe(η^5-C_5H_5)(η^5-C_5H_4-)}$_3$COH]≡[Fc_3COH]. However this has not been reported despite [Fc_3COH] being first prepared in 1962 [47] and studied intensively more recently [36,39,48], though there have been investigations of the electrochemistry of other multiferrocenyl compounds [45,49]. We were able to carry out our comparison because of a gift of [Fc_3COH]. The cyclic voltammograms of the two compounds, recorded in CH_2Cl_2 solution under identical sweep conditions, are illustrated in Fig. 14. The oxidations of the first two ferrocenyl groups of [Fc_3COH] ($E^0 = 0.47$, 0.66 V; $\Delta E_{ox} = 190$ mV) occur at potentials similar to those of **9** ($E^0 = 0.49$, 0.69 V; $\Delta E_{ox} = 200$ mV). Application of increased anodic potential to $[Fc_3COH]^{2+}$ generates the distinctive adsorption/stripping waveform. This is a consequence of low solubility of the salts of the multiply charged cation and resultant precipitation on the electrode surface. Reversal of the potential regenerates soluble species which redissolve, and thus repeat scans overlay. Similar behaviour has been observed for terferrocene [49] and ferrocenyl polyesters [50] when using the low polarity solvent CH_2Cl_2 and $[Bu_4N][PF_6]$ supporting electrolyte. In both of these cases, substitution of $[PF_6]^-$ with the large and weakly coordinating fluorinated aryl borate counter anion, $[B(C_6F_5)_4]^-$ [49] brought about normal solution-based, diffusion controlled electrochemical behaviour. We have not performed the cyclic voltammetry of triferrocenylcarbinol with the Geiger anion, but predict a similar result. In contrast, the triply charged $\mathbf{9}^{3+}$ cation remains in the CH_2Cl_2 solution even in the presence of the $[Bu_4N][PF_6]$ supporting electrolyte. We suggest that the bulky tetraphenylcyclobutadiene ligand interferes with the formation of the solid salt on the electrode surface.

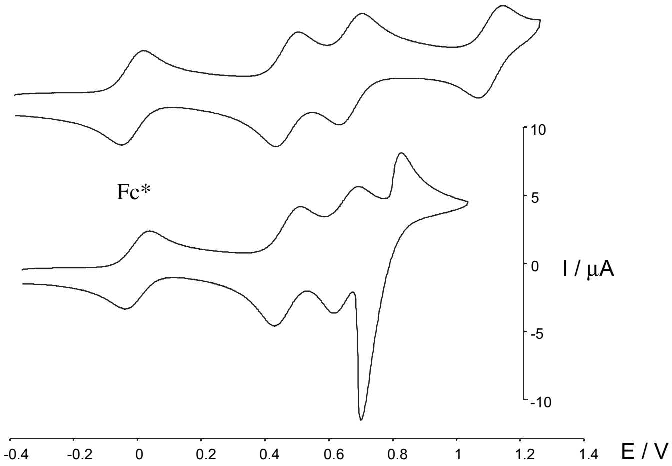

Fig. 14. Cyclic voltammograms of **9** (upper) and Fc_3COH (lower) in CH_2Cl_2 solution; 0.1 M $[Bu_4N][PF_6]$/100 mV s^{-1}/internal $[Fe(\eta^5\text{-}C_5Me_5)_2]^{+/0}$ reference (Fc*).

Cyclic voltammetry shows that in dichloromethane solution [**14**][BF_4] undergoes a quasi-reversible reduction to the [**14**]$^\cdot$ radical ($E^0 = -0.28$ V, $i_{pa}/i_{pc} = 0.2$). It also showed multiple oxidations on application of an anodic potential > 0.5 V, but these species were unstable and could not be characterised. [Fc_3C][BF_4] also underwent a reduction to its radical ($E^0 = -0.27$ V) but this was chemically reversible as was an oxidation at 0.96 V. For both [**14**][BF_4] and [Fc_3C][BF_4] salts the decamethylferrocene reference was non-innocent and gave rise to broad features between 0.5 and 0.7 V in the votammograms. This is the region for the oxidation of the alcohol precursors **9** and [Fc_3COH] which suggests that the cations decompose to neutral species.

4. Conclusions

The previously reported and readily prepared ester **2** and aldehyde **3** are shown to be excellent precursors for the preparation of other [Co(η^4-C_4Ph_4)(η^5-C_5H_4R)] complexes. The Co(η^4-C_4Ph_4)(η^5-C_5H_4–) radical is sufficiently robust to withstand the chemical demands made on it during our transformations, the products are air-stable, and the reactions are specific to the η^5-C_5H_4R ligand and do not appear to affect other parts of the molecules e.g. the phenyl groups.

The diethylphosphonate **6** and the triphenyl phosphonium salt [**7**]Cl are particularly useful synthons. In another paper from these laboratories they are used in the Horner–Wadsworth–Emmons or Wittig reactions to prepare functionalised alkenes of the general type [Co(η^4-C_4Ph_4)(η^5-$C_5H_4CH{=}CHR$)]. Furthermore, **6** has the potential to be a ligand in its own right (cf. Ref. [51]) and the precursor to the phosphonic acid [Co(η^4-C_4Ph_4)(η^5-$C_5H_4CH_2PO_3H_2$)] which could be used to prepare metal-organometallic arrays.

The alcohols **12** and **9** contain ferrocenyl as well as Co(η^4-C_4Ph_4)(η^5-C_5H_4-) groups. They are analogues of Ph_2CHOH, Fc_2CHOH, Ph_3COH and Fc_3COH and like them are precursors of stable cations i.e. [**13**]$^+$ and [**14**]$^+$ which were isolated as their $[BF_4]^-$ salts. As well as being analogues of diaryl and triarylmethyl cations, [**13**]$^+$ and [**14**]$^+$ could be used as precursors of other [Co(η^4-C_4Ph_4){η^5-C_5H_4CH(Fc)X}] and [Co(η^4-C_4Ph_4)(η^5-$C_5H_4CFc_2X$)] complexes where the hydroxyl groups have been replaced by different groups X (cf. ref. [36]). This would open the way to the incorporation of the chiral {Co(η^4-C_4Ph_4)(η^5-C_5H_4)}(Fc)(H)C- and bulky {Co(η^4-C_4Ph_4)(η^5-C_5H_4)}(Fc)$_2$C- moieties into molecules with possible applications in asymmetric syntheses, chiral catalysis and non-symmetric molecular machines. On the basis of our observations, it is reasonable to suggest that the Co(η^4-C_4Ph_4)(η^5-C_5H_4) group would confer a degree of oxidative (air) and thermal stability on such systems.

The electrochemical studies show that [Co(η^4-C_4Ph_4)(η^5-C_5H_4R)] complexes are always more difficult to oxidise than their ferrocenyl counterparts, and that in most instances the oxidation is not fully reversible. This resistance to oxidation may well be an advantage in situations such as those described above.

Acknowledgements

We thank the New Economy Research Fund (grant No. UOO-X0808) for support of this work (CJM). We are also grateful to

Professor Holger Butenschön (Leibniz Universität Hannover, Institut für Organische Chemie) for a sample of triferrocenylcarbinol allowing us to provide the first report of its electrochemical behaviour and to make comparison with the cobalt sandwich analogue reported herein.

Appendix A. Supplementary material

CCDC 798676–798685 contain the supplementary crystallographic data for this paper. These data can be obtained free of charge from The Cambridge Crystallographic Data Centre via www.ccdc.cam.ac.uk/data_request/cif.

Supplementary data associated with this article can be found, in the online version, at doi:10.1016/j.jorganchem.2010.12.026.

References

[1] A. Nakamura, N. Hagihara, Bull. Chem. Soc. Jpn. 34 (1961) 452.

[2] (a) J.S. Cannon, S.F. Kirsch, L.E. Overman, J. Am. Chem. Soc. 132 (2010) 15185;
(b) E. Bergin, D.L. Hughes, C.J. Richards, Tetrahedron: Asymmetry 21 (2010) 1619;
(c) A. Rodrigues, E.E. Lee, R.A. Batey, Org. Lett. 12 (2010) 260;
(d) A. Geny, N. Agenet, L. Iannazzo, M. Malacria, C. Aubert, V. Gandon, Angew. Chem. Int. Ed. 48 (2009) 1810.

[3] M.E. Mulcahy, Z. Bastl, K.F. Stensrud, T.F. Magnera, J. Michl, J. Phys. Chem. C 114 (2010) 14050.

[4] K. Nikitin, Y. Ortin, H. Müller-Bunz, M.-A. Plamont, G. Jaouen, A. Vessières, M.J. McGlinchey, J. Organomet. Chem. 695 (2010) 595.

[5] M.D. Rausch, R.A. Genetti, J. Org. Chem. 35 (1970) 3888.

[6] M.D. Rausch, R.A. Genetti, J. Am. Chem. Soc. 89 (1967) 5502.

[7] W.P. Hart, D.W. Macomber, M.D. Rausch, J. Am. Chem. Soc. 102 (1980) 1196.

[8] (a) A.M. Stevens, C.J. Richards, Organometallics 18 (1999) 1346;
(b) A.M. Stevens, C.J. Richards, Tetrahedron Lett. 38 (1997) 7805.

[9] H.V. Nguyen, M.R. Yeamine, J. Amin, M. Motevalli, C.J. Richards, J. Organomet. Chem. 693 (2008) 3668.

[10] P. O'Donohue, S.A. Brusey, C.M. Seward, Y. Ortin, B.C. Molloy, H. Müller-Bunz, A.R. Manning, M.J. McGlinchey, J. Organomet. Chem. 694 (2009) 2536.

[11] Y. Ortin, K. Ahrenstorf, P. O'Donohue, D. Foede, H. Müller-Bunz, P. McArdle, A.R. Manning, M.J. McGlinchey, J. Organomet. Chem. 689 (2004) 1657 and references therein.

[12] D. Seyferth, J.S. Merola, J. Organomet. Chem. 160 (1978) 275.

[13] (a) S. Barlow, S.R. Marder, in: T.J.J. Müller, U.H.F. Bunz (Eds.), Functional Organic Materials, Wiley-VCH, Weinheim, 2005, pp. 393–437;
(b) S.R. Forrest, M.E. Thompson (Eds.), Special Issue on Organic Electronics and Optoelectronics, Chem. Rev. 107 (2007) 923–1386.

[14] P. O'Donohue, C.J. McAdam, D. Courtney, Y. Ortin, H. Müller-Bunz, A.R. Manning, M.J. McGlinchey, J. Simpson, J. Organomet. Chem., in press.

[15] R. Jana, M.S. Kumar, N. Singh, A.J. Elias, J. Organomet. Chem. 693 (2008) 3780.

[16] D. Guillaneux, H.B. Kagan, J. Org. Chem. 60 (1995) 2502.

[17] J.N. Hay, J.F. McCabe, J.C. Robb, J. Chem. Soc. Faraday Trans. 1 68 (1972) 1.

[18] I. Noviandri, K.N. Brown, D.S. Fleming, P.T. Gulyas, P.A. Lay, A.F. Masters, L. Phillips, J. Phys. Chem. B 103 (1999) 6713.

[19] Note: different methods were used to generate LiFc in 2.4 and 2.7. Hindsight suggests that the Kagan method used in 2.4 (ref. 16) is the more appropriate of the two.

[20] SADABS. Bruker AXS Inc, Madison, WI 53711, 2000.

[21] G.M. Sheldrick, Acta Crystallogr. A64 (2008) 112.

[22] P. McArdle, J. Appl.Cryst. 28 (1995) 65.

[23] C.F. Macrae, P.R. Edgington, P. McCabe, E. Pidcock, G.P. Shields, R. Taylor, M. Towler, J. van de Streek, J. Appl.Cryst. 39 (2006) 453.

[24] J. Classen, R. Gleiter, F. Rominger, Eur. J. Inorg. Chem. 8 (2002) 2040.

[25] W.S. Wadsworth Jr., Org. React. 25 (1977) 73.

[26] O. Oms, F. Maurel, F. Carré, J. Le Bideau, A. Vioux, D. Leclercq, J. Organomet. Chem. 689 (2004) 2654.

[27] A. Michaelis, R. Kaehne, Chem. Ber. 31 (1898) 1048.

[28] S.T. Mabrouk, M.D. Rausch, J. Organomet. Chem. 523 (1996) 111.

[29] E. Knoevenagel, Chem. Ber. 31 (1898) 2596.

[30] M.D. Rausch, E.O. Fischer, H. Grubert, J. Am Chem. Soc. 82 (1960) 76.

[31] J.K. Lindsay, C.R. Hauser, J. Org. Chem. 22 (1957) 355.

[32] A.M. Asiri, Appl. Organomet. Chem. 15 (2001) 907.

[33] This work.

[34] Spectral Database for Organic Compounds, SDBS. National Institute of Advanced Industrial Science and Technology (AIST), Japan, 2010.

[35] C. Behrendt, S. Dabek, J. Heck, D. Courtney, A.R. Manning, M.J. McGlinchey, H. Müller-Bunz, Y. Ortin, J. Organomet. Chem. 691 (2006) 1183.

[36] J.R. Garabatos-Perera, R. Wartchow, H. Butenschön, J. Organomet. Chem. 689 (2004) 3541.

[37] R. Gleiter, H. Schimanke, S.J. Silverio, M. Büchner, G. Huttner, Organometallics 15 (1996) 5635.

[38] R. Rathore, C.L. Burns, I.A. Guzei, J. Org. Chem. 69 (2004) 1524.

[39] S. Cohen, J. Ma, H. Butenschön, R.H. Herber, Dalton Trans. (2009) 6606.

[40] L. Routaboul, J. Chiffre, G.G.A. Balavoine, J.-C. Daran, E. Manoury, J. Organomet. Chem. 637 (2001) 364.

[41] W. Zhang, Y. Yoneda, T. Kida, Y. Nakatsuji, I. Ikeda, J. Organomet. Chem. 574 (1999) 19.

[42] U. Koelle, Inorg. Chim. Acta 47 (1981) 13.

[43] E.V. Mutseneck, D.A. Loginov, D.S. Perekalin, Z.A. Starikova, D.G. Golovanov, P.V. Petrovskii, P. Zanello, M. Corsini, F. Laschi, A.R. Kudinov, Organometallics 23 (2004) 5944.

[44] F. Barrière, W.E. Geiger, J. Am. Chem. Soc. 128 (2006) 3980.

[45] G. Ferguson, C. Glidewell, G. Opromolla, C.M. Zakaria, P. Zanello, J. Organomet. Chem. 517 (1996) 183.

[46] F. Delgado-Pena, D.R. Talham, D.O. Cowan, J. Organomet. Chem. 253 (1983) C43.

[47] P.L. Pauson, W.E. Watts, J. Chem. Soc. (1962) 3880.

[48] J.R. Garabatos-Perera, H. Butenschön, J. Organomet. Chem. 693 (2008) 357.

[49] N. Camire, U.T. Mueller-Westerhoff, W.E. Geiger, J. Organomet. Chem. 637–639 (2001) 823.

[50] A. Nafady, C.J. McAdam, A.M. Bond, S.C. Moratti, J. Simpson, J. Solid State Electrochem. 13 (2009) 1511.

[51] S.R. Alley, W. Henderson, J. Organomet. Chem. 637–639 (2001) 216.